Structural Studies of Peptides and Polypeptides in the Solid State by Nitrogen-15 NMR

A. SHOJI,* S. ANDO,[†,‡] S. KUROKI,[†] I. ANDO[†] and G.A. WEBB[§]

**Department of Biological Sciences, Gunma University, Tenjin-cho, Kiryu-shi, Gunma 376, Japan*
[†]*Department of Polymer Chemistry, Tokyo Institute of Technology, Ookayama, Meguro-ku, Tokyo 152, Japan*
[§]*Department of Chemistry, University of Surrey, Guildford, Surrey, UK*
[‡]Present Address: *NTT Interdisciplinary Research Laboratories, Midori-cho, 3-Chome, Musashino-shi, Tokyo 180, Japan*

1. INTRODUCTION

The investigation of peptides, proteins and other biopolymers in the solid state is being increasingly pursued by means of NMR studies. This important area of scientific investigation regularly merits mention in three chapters of the *Specialist Periodical Reports on NMR*, namely those relating to solid-state NMR, synthetic macromolecules and natural macromolecules. The plethora of references contained in these reports leave little doubt as to the importance of solid-state NMR studies to the various areas of science in which peptides and related species play a key role.

The present review concentrates on the uses of nitrogen NMR studies in the structural investigations of peptides and similar compounds. Many of the molecules of interest are insufficiently soluble to permit solution-state NMR studies and thus solid-state measurements are the method of necessity. An

ANNUAL REPORTS ON NMR SPECTROSCOPY
VOLUME 26 ISBN 0-12-505326-6

additional virtue of solid-state NMR is that it provides the possibility of obtaining special information which the tumbling motion of molecules in a solution would average out. Analysis of orientation-dependent data obtained from solid-state NMR measurements, such as dipolar coupling between nitrogen and neighbouring nuclei and the nitrogen chemical shielding anisotropy (CSA) can provide an insight into molecular structure. Oriented molecules, in general, have NMR spectra which are very sensitive to changes in orientation with respect to the direction of the applied magnetic field. Thus, small changes in molecular orientation normally produce readily observable changes in the NMR signal splitting arising from CSA or dipolar coupling.

In order to be able to interpret such NMR spectra in terms of the molecular orientations it is necessary to have an accurate knowledge of the principal values and orientation of the chemical shielding or dipolar tensors in the molecule of interest. The experimental procedures used to determine these and related data are reviewed in Section 2. The following section, 3, deals with some possible theoretical interpretations of the shielding tensor and its principal components. Sections 4 and 5 cover applications of nitrogen NMR measurements to studies on oligopeptides and synthetic polypeptides respectively. The majority of the reports mentioned deal with ^{15}N NMR investigations. The additional quadrupolar signal-broadening produced by ^{14}N NMR is often counterproductive to the work which forms the main focus of this review.

2. EXPERIMENTAL PROCEDURES

2.1. Static measurements

2.1.1. Single-crystal measurements

The CSA is an unsymmetric nuclear spin interaction represented by a second rank Hermitian tensor. The anisotropy originates from the unsymmetric spatial distribution of electrons surrounding the observed nucleus. However, since the contribution from the antisymmetric parts can be neglected, the symmetric components of the CSA tensor can always be diagonalized. The CSA tensor is, therefore, characterized by the three principal values $(\sigma_{11}, \sigma_{22}, \sigma_{33})$ (σ_{11}, σ_{22} and σ_{33} are defined to be from high to low frequency in this review article) and their principal axis directions, which forms a principal axis system (PAS).[1,2] The observed chemical shieldings (σ_{obs}) of nuclei are displaced according to the orientation of the applied magnetic field with respect to the PAS of the CSA.

The angular dependence of the CSA interaction is given by

$$\sigma_{obs} = \sigma_{11} \cos 2\alpha \sin 2\beta + \sigma_{22} \sin 2\alpha \sin 2\beta + \sigma_{33} \cos 2\beta \qquad (1)$$

where α and β are the Euler angles which express the relative directions of the PAS with respect to the direction of the applied magnetic field. From the

rotation plots of the chemical shielding line positions the principal values and the direction of the chemical shielding tensor can be determind.[1–3]

2.1.2. *Polycrystalline measurements*

Large single crystals of peptides, necessary for single-crystal measurements, are usually not available because they are difficult to grow. For polycrystalline samples, the NMR spectrum becomes the sum of single-crystal spectra for all directions, the so-called "powder pattern".

According to the calculation of Bloembergen and Rowland,[4] the intensity of the NMR signal at the frequency ω is expressed as

$$I(\omega) = \pi^{-1}(\omega - \omega_{11})^{-1/2}(\omega_{33} - \omega_{22})^{-1/2}K(m) \tag{2}$$

for

$$\omega_{33} > \omega > \omega_{22}$$

where

$$m^2 = (\omega_{22} - \omega_{11})(\omega_{33} - \omega)/(\omega_{33} - \omega_{22})(\omega - \omega_{11}) \tag{3}$$

$$I(\omega) = \pi^{-1}(\omega_{33} - \omega)^{-1/2}(\omega_{22} - \omega_{11})^{-1/2}K(m) \tag{4}$$

for

$$\omega_{22} > \omega > \omega_{11}$$

where

$$m^2 = (\omega - \omega_{11})(\omega_{33} - \omega_{22})/(\omega_{33} - \omega)(\omega_{22} - \omega_{11}) \tag{5}$$

and

$$I(\omega) = 0 \quad \text{in case } \omega > \omega_{33} \text{ and } \omega < \omega_{11}$$

where $K(m)$ is the complete elliptic integral of the first kind as

$$K(m) = \int_0^{\pi/2} (1 - m^2 \sin^2 \phi)^{-1/2} \mathrm{d}\phi \tag{6}$$

The principal values of the shielding tensor $(\sigma_{11}, \sigma_{22}, \sigma_{33})$ can be obtained directly from the powder pattern but no information is obtained about the orientation of the shielding tensor. The orientation can be determined from a single-crystal study, theoretical calculation, symmetrical consideration, or from related compounds whose tensor orientations are already determined.

As shown in Fig. 1, a typical ^{15}N powder pattern of a peptide reveals axial symmetry because the electronic structure around the nitrogens of the peptide bonds is nearly symmetrical around the axes of the N–H bonds. In such cases, the orientation of the principal axis is difficult to determine even from a single-crystal study. The directions of the two principal values, σ_{11} and σ_{22}, are determined by using the dipolar interactions between the nitrogen and the adjacent

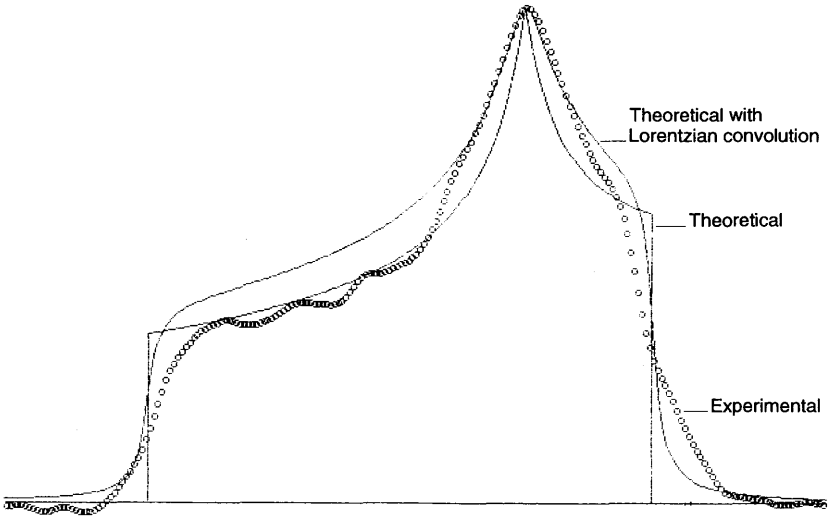

Fig. 1. Schematic representation of experimental powder pattern and theoretical powder pattern and theoretical powder pattern convoluted with the Lorentzian function. The circles indicates the experimental data for glycylglycine · HNO_3. (S. Kuroki and I. Ando, unpublished data.)

carbonyl carbon nucleus. Another problem in this experiment is that the background signal due to unenriched sites often contributes to the skirts of the powder pattern spectrum. Even though the nitrogen of interest is enriched, the two principal values read off from the outer regions, σ_{11} and σ_{33}, are likely to contain some errors.

2.2. Cross-polarization/magic-angle spinning and double cross-polarization NMR measurements

2.2.1. ^{15}N *cross-polarization/magic-angle spinning NMR method*

Since the ^{15}N nucleus has spin-$\frac{1}{2}$ but low natural abundance (0.365%) and a low magnetogyric ratio ($\gamma = -2.7126 \times 10^7$ rad/s T) and so a rather low NMR sensitivity,[5–7] it is difficult to obtain a solid sample spectrum from a single pulse experiment. Recently, the cross-polarization/magic-angle spinning (CP/MAS) technique[1,2,8] has been applied to solid samples and thus we can obtain high-resolution NMR spectra from solids. The CP experiment involves polarization transfer from ^1H to dilute spin-$\frac{1}{2}$ nuclei such as ^{13}C or ^{15}N. The matching condition can be predicted from the Hartmann–Hahn condition as

$$\gamma_N \sigma B_N = \gamma_H \sigma B_H \tag{7}$$

where σB_N and σB_H are the magnetic fields for the ^{15}N and ^{1}H nuclei, respectively, in the rotating frame. When this matching condition is satisfied, the ^{15}N signal intensity is increased by $\gamma_H/\gamma_N = 9.86$ times. Magic-angle spinning removes the CSA. Since the CSA of a peptide amide nitrogen ^{15}N is about 3–5 kHz, the sample has to be spun at more than 4 kHz.

2.2.2. *^{1}H–^{13}C–^{15}N double CP NMR method*

The double CP experiment[9,10] involves the sequential transfer of polarization among three spin-$\frac{1}{2}$ systems. This technique can be used to observe selectively one type of spin (e.g. ^{15}N) which is directly bonded to another nucleus (e.g. ^{13}C). Since both ^{15}N and ^{13}C nuclei are rare spins, ^{13}C–^{15}N bonds are extremely rare occurrences in natural isotopic abundance peptides. The ^{13}C–^{15}N bonds observed in this experiment originate from doubly-labelled compounds. The different kinds of labelled ^{13}C–^{15}N bonds and their concentrations can be detected.

2.2.3. *Spinning sideband intensity method*

The NMR lineshapes observed in proton-decoupled ^{15}N spectra are dominated by the CSA. In the CP/MAS experiment, high resolution is achieved at the expense of the information contained in the anisotropy. But when the spinning frequency is less than the nuclear shielding anisotropy, the isotropic line in the NMR spectrum is flanked on both sides by sidebands spaced at the spinning frequency. Maricq and Waugh[11,12] have shown that the second and third moments of the NMR spectra can be used to extract the shielding anisotropy from the sideband intensities. Herzfeld and Berger[13] have derived general integral and series expansions for sideband intensities. Principal values of the shielding tensor can be derived from the intensities of a relatively small number of sidebands. An example of this experiment for glycylglycine · HNO_3 is shown in Fig. 2. The sample was spun 1.6 kHz, and three principal values of the components of the shielding tensor are obtained as $\sigma_{11} = 197$ ppm, $\sigma_{22} = 52$ ppm and $\sigma_{33} = 21$ ppm.

2.2.4. *Dipolar NMR method*

In the simple CP/MAS experiment for ^{15}N and ^{13}C nuclei in a peptide, scalar coupling to ^{1}H is not observed because high-power ^{1}H decoupling is used to remove the ^{1}H–^{15}N or ^{1}H–^{13}C dipolar interactions. However, for the carbons directly bonded to nitrogens, ^{14}N–^{13}C or ^{15}N–^{13}C dipolar interactions are not averaged out by MAS and broadened asymmetric doublets are observed.[14–17] Accord-

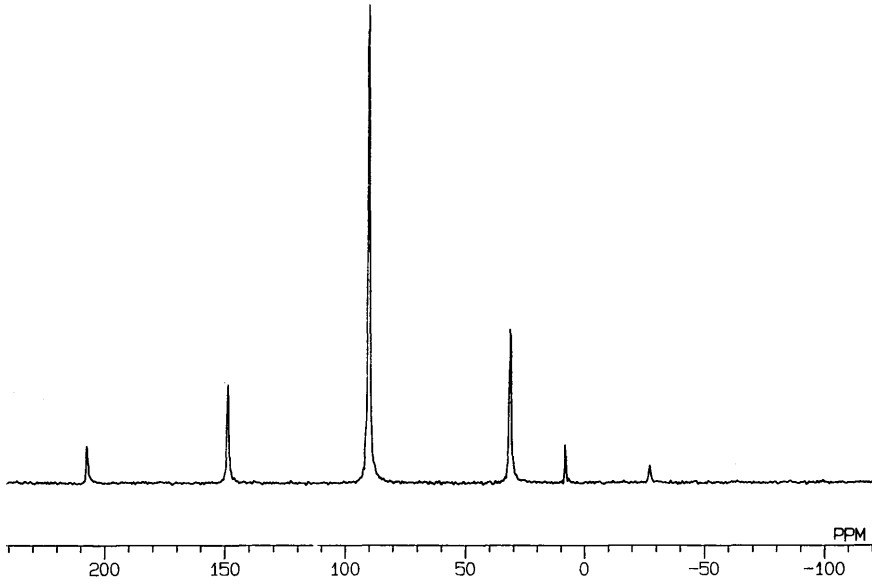

Fig. 2. The 27.3-MHz ^{15}N CP/MAS NMR spectrum of glycylglycine · HNO_3 in the solid state. The magic-angle spinning rate is 1.6 kHz. (S. Kuroki and I. Ando, unpublished data.)

ing to the scheme expressed by Linder *et al.*,[14] the powder pattern spectrum, $S(v)$, of a dipolar-coupled nuclear site can be expressed in the following form:

$$S(v) = \sum_i s(v_i) = \sum_i \int_{\theta=0^\circ}^{180^\circ} \int_{\phi=0^\circ}^{360^\circ} g_i[v, v_i(\theta, \phi, \alpha_D, \beta_D)] \sin\theta \, d\theta \, d\phi \qquad (8)$$

where θ and ϕ are polar angles which describe the orientation of the chemical shielding PAS with respect to the magnetic field fixed in the laboratory frame;

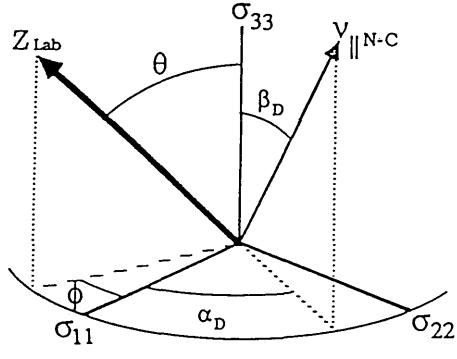

Fig. 3. The orientation of the N–C_1 internuclear vector ($v_{\|N-C}$) with respect to the shielding tensor (σ_{ii}) is given by α_D and β_D. The orientation of the laboratory Z axis (Z_{Lab}) with respect to the shielding tensor is given by θ and ϕ.

α_D and β_D are rotations which transform the dipolar interaction into the PAS of the shielding tensor (Figs 3 and 4), v is the observed frequency, and $v_i(\theta, \phi, \alpha_D, \beta_D)$ is the transition frequency for a particular orientation of the shielding and dipolar tensors.

On the other hand, the dipolar coupled signal of nitrogen is observed when the carbons directly bonded to nitrogen are labelled by ^{13}C or when the hydrogens are not decoupled.[18] The double labelling of the peptide nitrogen and carbon with ^{15}N and ^{13}C is, however, frequently used to extract information about the orientation of the N–C bond because a principal axis of the dipolar tensor always coincides with that of the C–N bond.[19] The dipolar interactions between nitrogen (^{14}N and ^{15}N) and hydrogen have been studied to obtain the bond lengths of N–H bonds.[20,21]

3. THEORETICAL INTERPRETATION OF NITROGEN NMR SHIELDINGS

The general principles involved in calculations of NMR nuclear shieldings from quantum mechanical considerations have been described elsewhere.[22] Only a very brief summary of the available types of shielding calculation likely to be relevant to peptides and polypeptides is given here. Normally, for large molecules semi-empirical molecular orbital (MO) procedures are employed for nuclear shielding calculations. This contrasts with the situation for smaller molecules, containing a maximum of about 11 heavy atoms, for which *ab initio* MO methods can produce very satisfactory estimates of nuclear shielding.[23] Progress in nuclear shielding calculations forms the basis of an annual report.[24] Nuclear shieldings are determined by the molecular environment in which the nucleus finds itself. Thus the effectiveness of a MO calculation of nuclear shielding depends on the success of the procedure used in describing the molecular electronic environment. Commonly used procedures provide estimates of the major shielding contributions, namely the diamagnetic and paramagnetic contributions which usually have opposite signs. For a given

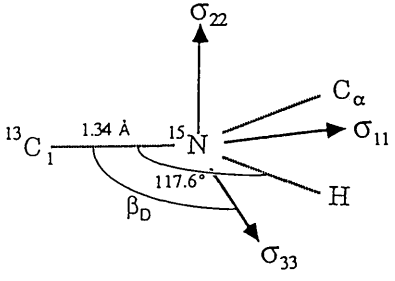

Fig. 4. Orientation of the shielding tensor elements in the molecular frame on alanylalanine, σ_{11} lies essentially in the plane of the peptide linkage as do the N–H, N–C_α, and N–C_1 bonds.

type of nucleus, such as nitrogen, in a variety of electronic environments the diamagnetic contribution to the change in shielding is usually about 3% or less of the total change. Consequently, it is the paramagnetic contribution which controls the variation of nuclear shielding with environment. Unfortunately, this is the more difficult of the two types of contributions to calculate reliably.

Both the sum-over-states (SOS) and finite perturbation theory (FPT) have been widely employed to estimate the diamagnetic and paramagnetic shielding contributions for molecules of various sizes. The SOS approach requires an accurate knowledge of the molecular excited states and their excitation energies. This can be difficult to obtain by self-consistent field (SCF) MO methods, in particular by semi-empirical MO procedures. In contrast the FPT approach has the advantage of not requiring explicit wavefunctions for the excited states. The FPT-INDO method has been successfully used in nitrogen shielding calculations on *N*-methylacetamide which has been employed as a model compound in conjunction with nitrogen NMR spectra taken on a variety of solid oligopeptides, (X–Gly–Gly)[25] and (Boc–Gly).[26] The importance of *ab initio* nitrogen shielding calculations, using an individual gauge for localized molecular orbitals (IGLO) and the localized orbital local origins (LORG) methods, has been discussed in a review.[27] In general these procedures can provide satisfactory estimates of nitrogen shielding tensors for small molecules. IGLO calculations have been reported for DNA bases with some success.[28] Similar calculations on some model peptides could be of interest. It should be recognized that the results of MO calculations on monomeric species may not be readily transferable to polymers. This arises from the fact that in small molecules the electrons are confined to a finite region of space whereas this may not be the case for polymers. Consequently calculations of polymer electronic structure require the inclusion of long range and interchain interactions. These can be incorporated into calculations of nuclear shielding by means of the tight-binding (TB) procedure.[29]

Calculations of nuclear shielding normally provide values for each of the nine components of the second-order shielding tensor. Thus theoretical estimates are available for the principal components of the tensor as well as its anisotropy and the isotropic value of the nuclear shielding, the latter of which is usually available from high-resolution CP/MAS NMR measurements. Methods for experimentally determining the principal tensor components, and its anisotropy, are described in the previous section.

4. OLIGOPEPTIDES

4.1. Shielding tensors

In order to establish the orientation of a peptide backbone or side-chain residue from chemical interactions, the orientation of the shielding tensor in the molecular frame needs to be determined.

The ^{15}N shielding tensor of a peptide was first determined for L-histidine hydrochloride monohydrate from a single-crystal study by Harbison *et al.*[30] The principal components of the shielding of the imidazole ring nitrogens are oriented approximately along the molecular symmetry directions differing from them by only 3° and 5°, and the most shielded element, σ_{33}, is perpendicular to the plane of the imidazole ring.

The orientation of the ^{15}N shielding tensor in the amino group was determined for L-asparagine · H_2O from the sideband intensities in the ^{15}N–^{1}H dipolar/chemical shift spectrum by Herzfeld *et al.*[31] In the presence of magic-angle spinning, two-dimensional solid-state NMR spectra of magnetically dilute $I = \frac{1}{2}$ nuclei split into rotational sidebands spaced at the spinning frequency in both dimensions. The dipolar slice, corresponding to particular shift sidebands, is asymmetric and contains information regarding the relative orientations of the shielding and dipolar tensors. The calculated two-dimensional spectra for the six orientations are compared to the observed spectrum, and a good match is only obtained for that in which the quasi-unique component σ_{11} is perpendicular to the H–N–H disector in the H–N–H plane.

It is concluded that σ_{33} lies along the H–N–H bisector, σ_{22} lies perpendicular to the H–N–H plane, and σ_{11} lies in the H–N–H plane, perpendicular to the H–N–H bisector.

Through the observation of proton-decoupled ^{15}N NMR lineshapes of two crystalline phases of Boc-glycylglycyl[^{15}N,^{2}H]glycine benzyl ester, the ^{15}N–^{2}H bond length and the direction of the most deshielded component of the shielding tensor, σ_{11}, have been determined, combined with X-ray diffraction data.[32]

The ^{15}N shielding tensor of the amide group was examined for uniformly ^{15}N-labelled glycylglycine hydrochloride monohydrate, from the dipolar/chemical shift spectra produced by two-dimensional magic-angle NMR methods.[33] It is found that the nearly axially symmetric ^{15}N shielding tensor is tilted 25° away from the N–H bond. The same ^{15}N shielding tensor was determined for [1-^{13}C]glycyl[^{15}N]glycine hydrochloride monohydrate from a single-crystal study.[34] Although one of the components of the ^{15}N tensor is perpendicular to the plane of the peptide bond, the tensor is very close to being axially symmetric. The orientations of σ_{33} and σ_{22} could not be determined. The angle between the N–H bond vector and σ_{11} is 21.3°, which is larger than that of the imidazole nitrogen in histidine.

The ^{15}N–^{1}H dipolar/chemical shift spectra were observed for polycrystalline samples of [^{15}N]acetylvaline, α-[^{15}N]glycyl-[^{15}N]glycine, [^{15}N]glycyl-[^{15}N]glycine · HCl · H_2O, [^{15}N]acetyl-glycine, [π-^{15}N]-1-histidine · HCl · H_2O, and [ϵ-^{15}N]tryptophan[21] (Fig. 5).

The first four ^{15}N–^{1}H systems, all peptide linkages, yield similar results to [1-^{13}C]glycyl[^{15}N]glycine · HCl · H_2O where the σ_{11} principal axis of the shielding tensor is rotated approximately 20° from the unique principal axis

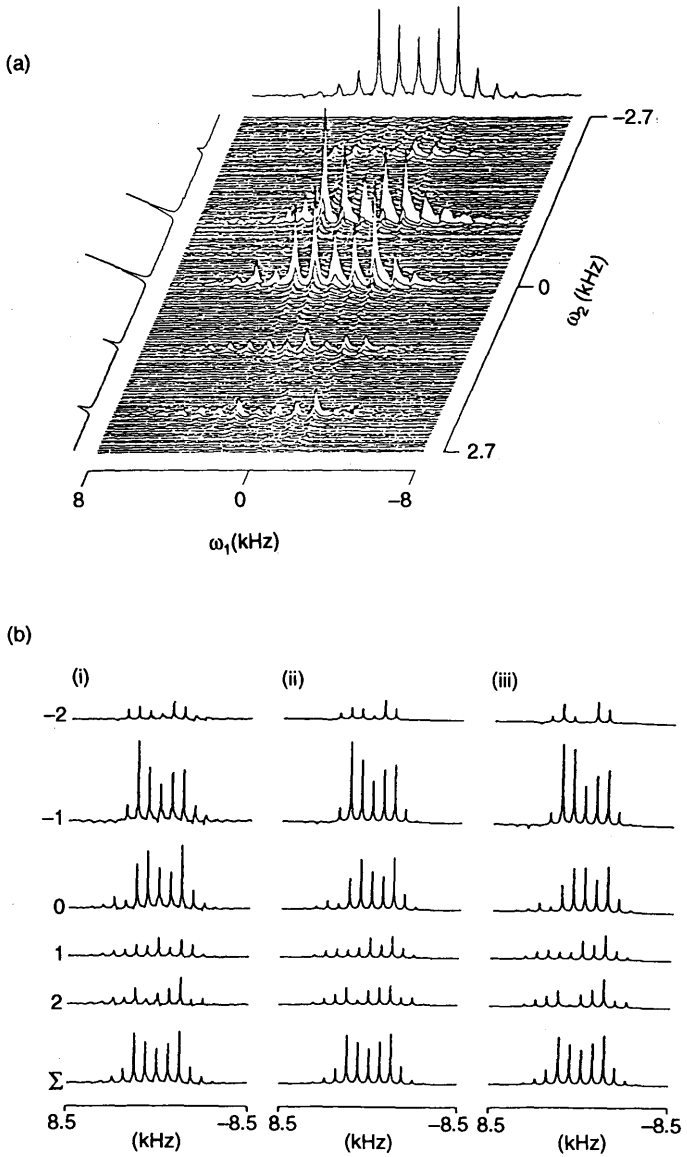

Fig. 5. (a) Two-dimensional ^{15}N–^{1}H dipolar/chemical shift spectrum obtained from [^{15}N]acetylvaline showing the dipolar and chemical shift projections. Linewidths are typically 50–150 Hz for the dipolar and 0.5–1.0 ppm for the chemical shift dimension. $\nu_R = 1.07$ kHz. (b) Dipolar cross-sections taken from the 2D spectrum. Each trace runs parallel to ω_1, through a particular rotational sideband in ω_2. (i) Experimental ^{15}N–^{1}H spectra from [^{15}N]acetylvaline, $\nu_R = 1.07$ kHz. The two simulations (ii and iii) assume two different orientations of the dipolar and shielding tensors, ($\beta_D = 22°$, $\alpha_D = 0°$) and ($\beta_D = 17°$, $\alpha_D = 0°$), respectively, and illustrate the subtle differences in orientation which can be detected in the spectra.

of the dipolar tensor. However, the location of the other two principal axes cannot be determined accurately because of the almost axial symmetry of the ^{15}N shielding tensor. In addition, the dipolar/chemical shift experiments yield a value of the length of the ^{15}N–^{1}H bond which is accurate to within 0.005 Å and the mutual orientations of the dipolar and shielding tensors accurate to within 3°. A comparison of the bond lengths obtained from NMR experiments with similar data from neutron diffraction experiments shows that the former is uniformly 0.0035 Å longer than the latter.

The dipolar-coupled ^{15}N shielding powder patterns contain enough information to allow the determination of the orientation of the dipolar vector (N–C or H–N bond) in the PAS of the shielding tensor. Hartzell *et al.*[35] have determined the orientation of the ^{15}N shielding tensor relative to the molecular frame for polycrystalline L-[1-^{13}C]alanyl-L-[^{15}N]alanine using a ^{1}H dipole-modulated, ^{13}C dipole-coupled ^{15}N spectrum (Fig. 6). The orientation of the ^{13}C–^{15}N bond to the most shielded component, σ_{33}, is 106°, in which the angle between the N–H bond and σ_{33} is 12°. In addition, the σ_{22} is perpendicular to the peptide plane, and σ_{11} is in the peptide plane perpendicular to σ_{22} and σ_{33}.

The ^{15}N shielding tensors of a homologous series of peptides of the form *N*-acetyl[1-^{13}C]glycyl[^{15}N]X-amide (X = glycine, L-alanine and tyrosine) and the unprotected dipeptide [1-^{13}C]glycyl[^{15}N]glycine hydrochloride have been determined from ^{13}C dipole-coupled ^{15}N powder patterns.[36,37] It is reported that the common shielding tensor orientation places σ_{22} perpendicular to the peptide plane, and σ_{33} at a 99° angle with respect to the C–N bond. The orientations of σ_{11} and σ_{22} were first determined for ^{15}N shielding tensors of amides, there are no significant differences in the molecular orientations of the tensors, although there are large lattice-dependent variations in the ^{15}N shielding tensor principal values.

On the other hand, the orientation of the σ_{33} component of the amide ^{15}N shielding tensor was determined from dipolar-coupled ^{15}N powder patterns by Teng *et al.*[38–40] (Fig. 7). Two doubly-labelled molecules, [1-^{13}C]glycyl$_2$[^{15}N]-alanyl$_3$-gramicidin-A and [1-^{13}C]alanyl$_3$[^{15}N]-D-leucyl$_4$-gramicidin-A, in a liquid environment were used, and the orientations of the ^{13}C–^{15}N bonds to the σ_{33} component are 104° and 105°, in which the angles between the N–H bond and σ_{33} range between 12° and 14°. These results are very close to those reported for alanylalanine by Hartzell *et al.* (12°),[35] but slightly deviate from other data by Oas *et al.* (20° ± 2°),[36] Munowitz *et al.* (25° ± 5°)[33] and Harbison *et al.* (21°).[34] It can be said that the orientation of the shielding tensor relative to the molecular frame is variable and consequently there is a need to determine the tensor orientation for each site of interest.

A rotational-echo, double-resonance (REDOR) ^{15}N–^{13}C NMR experiment has been performed on an alanine co-crystallized from five-component alanines, isotopically enriched in ^{13}C, ^{15}N, or ^{13}C.[41–43] REDOR ^{15}N–^{13}C NMR involves the dephasing of carbon magnetization by ^{15}N 180° pulses synchronized with magic-angle spinning. The C–N dipolar coupling deter-

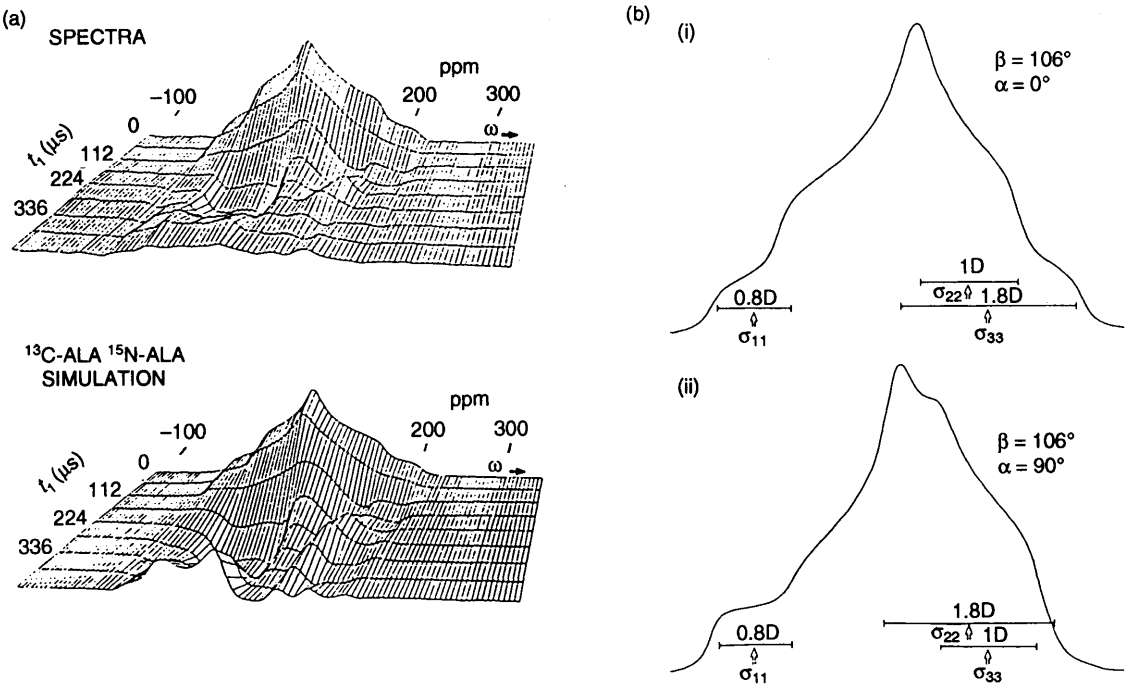

Fig. 6. (a) Transform in t_2 of the ^{1}H dipole-modulated, ^{13}C dipole-coupled, ^{15}N powder FID of [1-^{13}C]alanyl-[^{15}N]alanine. The number of MREV-8 cycles (56 μs) was increased from 0 to 8 during t_1. The frequency axis is reported in ppm relative to liquid NH_3 at −50°C. (b) Unmodulated simulations for two orientations of σ_{33} and σ_{22} relative to the peptide plane. (i) The orientation described by $\beta_{CN} = 106°$, $\alpha_{CN} = 90°$ places σ_{33} perpendicular to the plane and σ_{22} in the plane nearly parallel to the C–N bond. (ii) The orientation described by $\beta_{CN} = 106°$, $\alpha_{CN} = 90°$ places σ_{33} perpendicular to the plane and σ_{22} in the plane nearly parallel to the C–N bond.

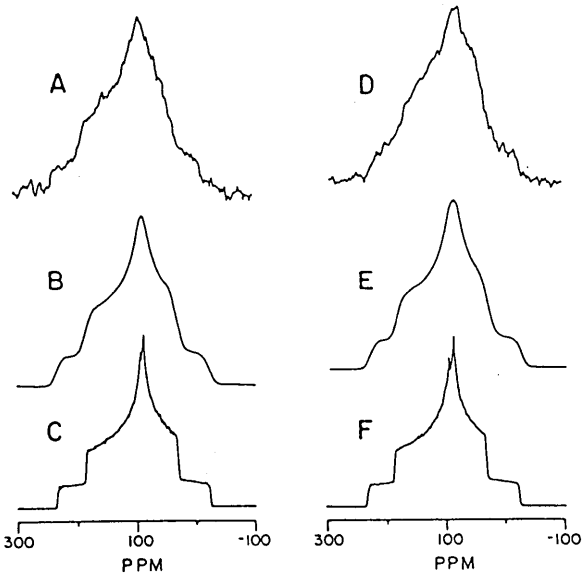

Fig. 7. Experimental (A and D) and theoretical (B < C < E and F) ^{15}N powder pattern spectra of doubly labelled gramicidin A. (A) Spectrum of [1-^{13}C]glycyl$_2$[^{15}N]alanyl$_3$-granicidin A with an observed dipolar splitting, $\Delta\nu_3 = 970$ Hz, indicating a β_D angle of 106°. (B) Broadened (360 Hz of Gaussian broadening) version of theoretical spectrum shown in C. (C) Theoretical spectrum yielding a best fit to the experimental data with $\alpha_D = 0°$ and $\beta_D = 104°$. (D) Spectrum of [1-^{13}C]alanyl$_3$-D-[^{15}N]leucyl$_4$-gramicidin A with an observed dipolar splitting, $\Delta\nu_3 = 1010$ Hz, indicating a β_D angle of 105°. (E) Broadened (360 Hz of Gaussian broadening) version of theoretical spectrum shown in (F). (F) Theoretical spectrum yielding a best fit to the experimental data with $\alpha_D = 0°$ and $\beta_D = 105°$.

mines the extent of dephasing. These experiments on alanine show that it is practical to use REDOR to measure the C–N dipolar coupling of 5 μmol of a ^{13}C–^{15}N-labelled pair having an internuclear separation of the order of 4.5 Å.

4.2. Isotropic chemical shifts

High-resolution ^{15}N CP/MAS NMR spectra of a variety of solid oligopeptides (X-glycylglycine) have been measured by Kuroki *et al.*[25] in order to clarify the relationship between the hydrogen bonding structure and ^{15}N shielding. It is found that there is no relationship between hydrogen bond length ($R_{N\cdots O}$) and Gly NH amide ^{15}N isotropic shielding (Fig. 8), but that the decrease of the N–H bond length (R_{N-H}) leads to a linear increase in ^{15}N isotropic shielding (Fig. 9). The expression for this relationship is

$$\delta_{obs} = 39.32R_{N-H} + 57.73 \text{ (ppm)}$$

In order to investigate the relationship between R_{N-H} and $R_{N\cdots O}$, quantum

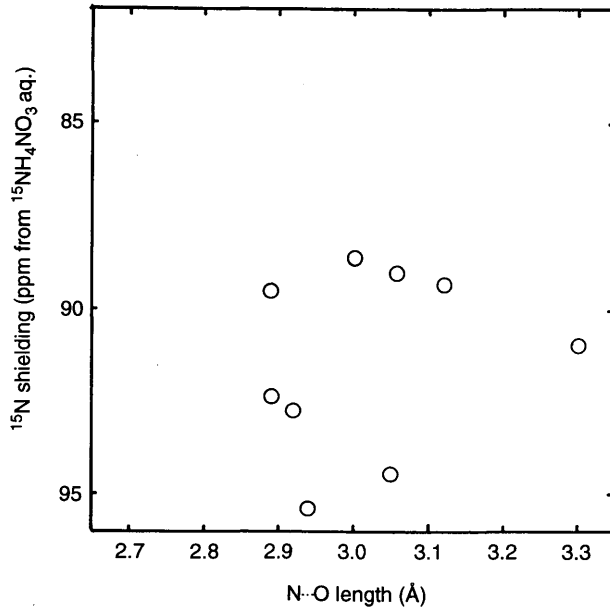

Fig. 8. Plot of the observed ^{15}N shielding of oligopeptides in the crystalline state against the N···O hydrogen bond length.

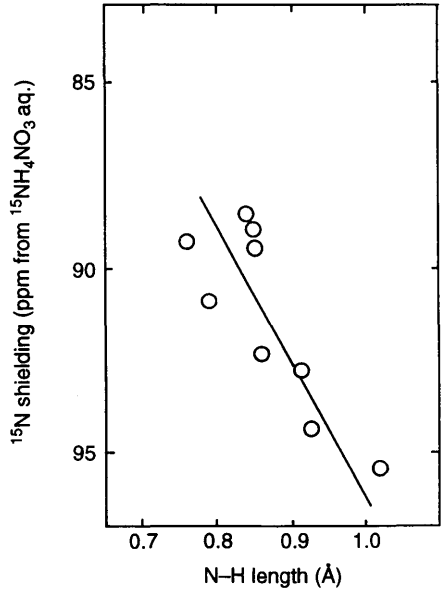

Fig. 9. Plot of the observed ^{15}N shielding of oligopeptides in the crystalline state against the N–H bond length.

chemical calculations were carried out using two hydrogen-bonded *N*-methyl acetamides. It is shown that at the region forming hydrogen bond, an increase of $R_{N\cdots O}$ leads to a decrease in R_{N-H} (Fig. 10). On the other hand, X-ray diffraction studies have shown that the R_{N-H} values decrease with an increase in the $R_{N\cdots O}$ values. Further, it is found that not only the hydrogen bond length but also the hydrogen bond angle ($\angle$N–H$\cdots$O) is related to the ^{15}N shielding. As shown in Section 3, ^{15}N shielding calculations were carried out using a model compound, by the FPT-INDO method; the calculated results reasonably explain the experimental ones in Fig. 11.

The relationship between amide nitrogen isotropic shielding and the principal values (σ_{11}, σ_{22}, and σ_{33}) of the shielding and hydrogen bond length $R_{N\cdots O}$ and hydrogen bond angle $\angle$N–H$\cdots$O has been studied by observing CP/MAS and CP/static ^{15}N NMR spectra of a variety of solid oligopeptides (*tert*-butyloxycarbonylglycyl-X).[25] From the results of the observed ^{15}N shieldings, it was found that the isotropic ^{15}N shieldings (σ_{iso}) of the glycine residues increase with an increase of hydrogen bond length ($R_{N\cdots O}$) between the nitrogen and oxygen atoms in the amide groups (Fig. 12), and that the principal values of σ_{33} decreases linearly with a decrease of $R_{N\cdots O}$ and there is no relationship between the principal values σ_{11}, σ_{22} and $R_{N\cdots O}$ (Fig. 13).

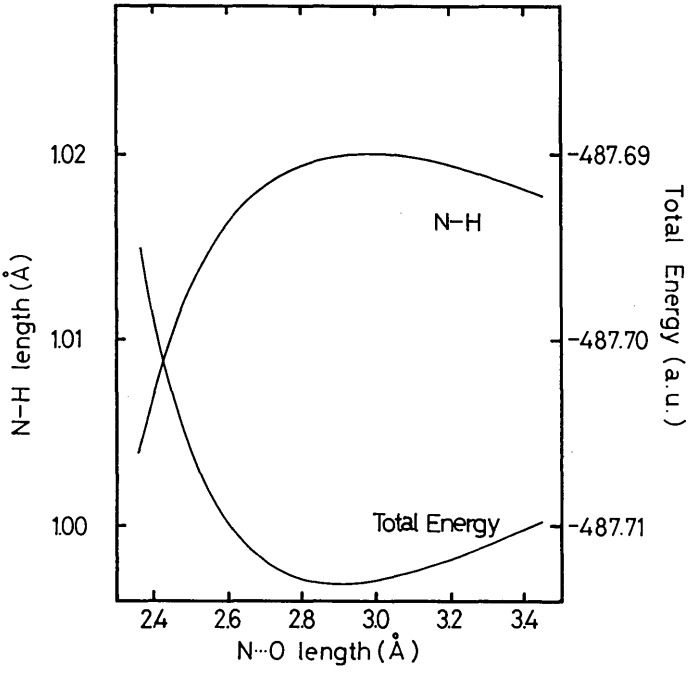

Fig. 10. Plot of the calculated N–H bond length and total energy against the hydrogen bond length (N$\cdots$O) obtained by using the *ab initio* STO-3G MO method.

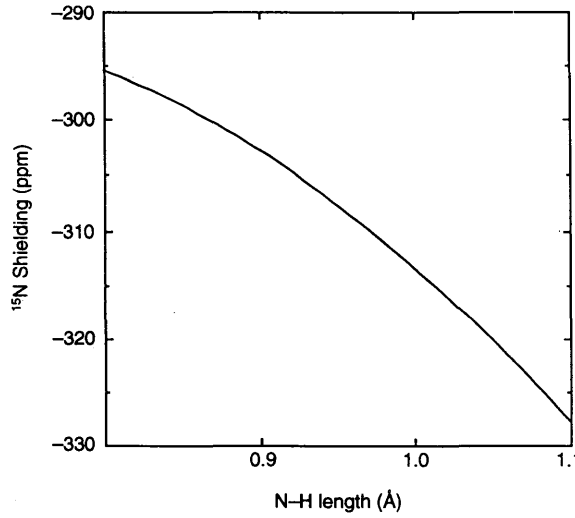

Fig. 11. Plot of the calculated ^{15}N shielding against the N–H bond length obtained from the FPT-INDO method.

As shown in Section 3, quantum chemical calculations of the ^{15}N shielding constant for the model compounds were carried out by the FPT-INDO method, and the relationship between ^{15}N shielding and $R_{N\cdots O}$, $\angle$N–H$\cdots$O was discussed (Figs 14 and 15). These results show that the σ_{11} and σ_{22} components are related not only to the hydrogen bond length ($R_{N\cdots O}$), but also to the hydrogen bond angle ($\angle$N–H$\cdots$O), but σ_{33} is related to the hydrogen bond

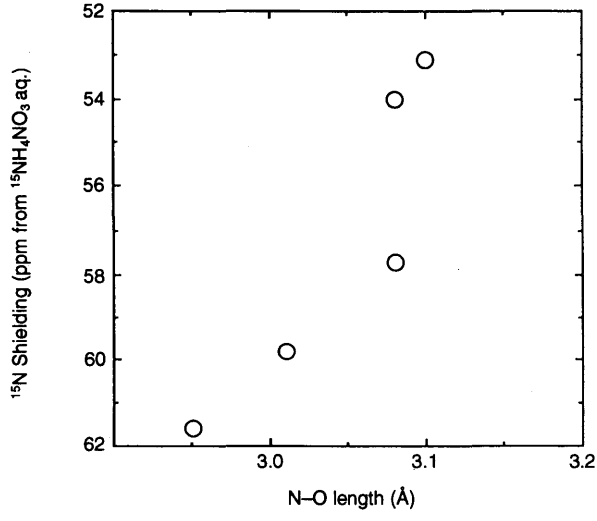

Fig. 12. Plot of the observed ^{15}N shielding in the solid state against the N$\cdots$O length.

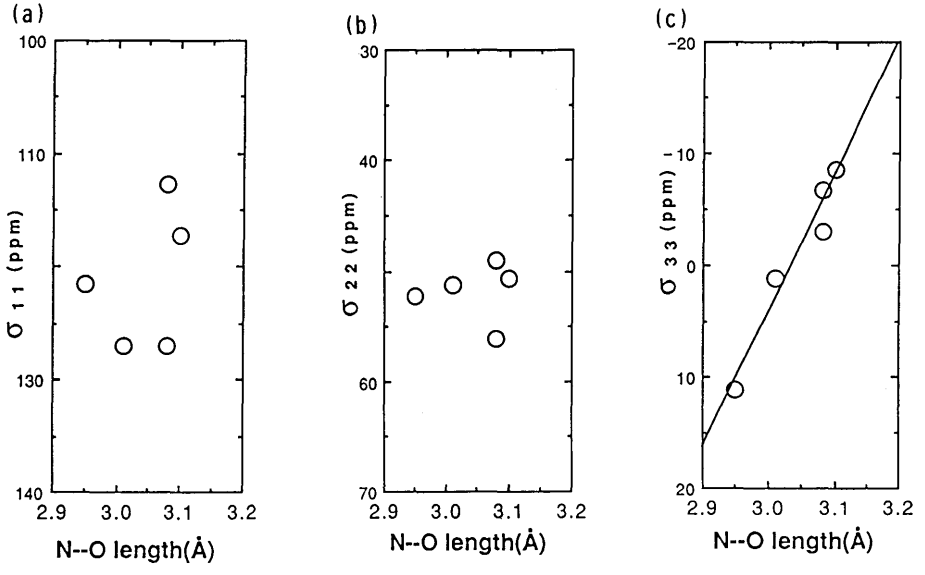

Fig. 13. Plots of the observed principal values of ^{15}N shielding tensors (a) σ_{11}, (b) σ_{22}, and (c) σ_{33} against the N···O bond length.

length ($R_{N\cdots O}$) only. Therefore, it can be said that the ^{15}N isotropic shielding and the three principal values of the shielding of the amide nitrogen provide useful information about the hydrogen bond length and hydrogen bond angle.

5. SYNTHETIC POLYPEPTIDES

High-resolution and solid-state ^{15}N NMR has been increasingly applied to the investigation of polypeptides, proteins and biopolymers.[30,44–59] This is because, especially in polypeptides and proteins, nitrogen is very often functionally important due to its ability to form hydrogen bonds, most of the nitrogen sites are in the amide linkage of the backbone and the structure and dynamics of the backbone strongly reflect the conformation and the flexibility of these macromolecules. Foerster *et al.*[47] have measured the ^{15}N CP/MAS NMR spectra of some synthetic polypeptides in the solid state and found that the isotropic ^{15}N chemical shift depends upon conformational features such as the secondary structure determined by the peptide bonds of the backbone. Shoji *et al.*[57–59] have studied systematically the relation between the ^{15}N chemical shifts and structure such as primary, secondary and higher ordered structures of various kinds of synthetic polypeptides in the solid state. They have demonstrated that the ^{15}N chemical shifts in the peptide backbone of these polypeptides change depending on conformation, nature of amino acid residue, amino acid sequence and manner of hydrogen bonding. It is noteworthy

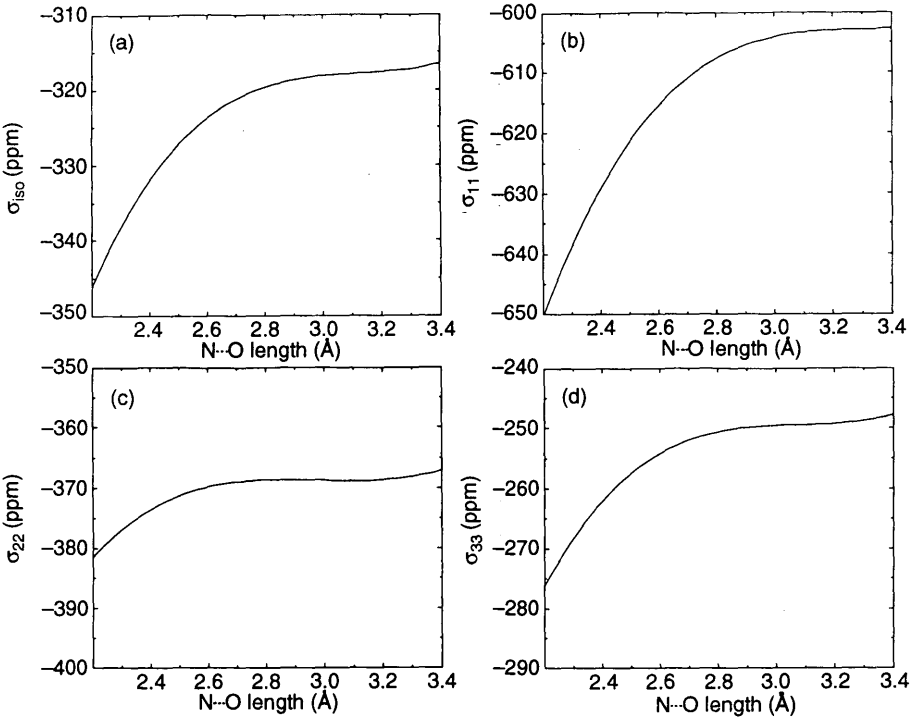

Fig. 14. Variation of the calculated ^{15}N shielding and its tensor components with the N···O hydrogen bond length: (a) σ_{iso}, (b) σ_{11}, (c) σ_{22}, and (d) σ_{33}.

that the ^{15}N shielding tensors are related to the structures of the solid polypeptides. Thus, it is now possible to determine the conformation of polypeptides and some proteins in the solid state by the ^{15}N CP/MAS NMR method. The NMR work is likely to become increasingly important in the study of the structure and dynamics of synthetic polypeptides and natural proteins in the solid state. Accordingly, if the sensitivity problem can be overcome, ^{15}N would be an ideal candidate for investigating polypeptides, proteins and biopolymers.

5.1. Isotropic ^{15}N chemical shifts

5.1.1. Homopolypeptides

Foerster *et al.*[47] measured the first ^{15}N CP/MAS NMR spectra of some ^{15}N-labelled homopolypeptides in the solid state. Figure 16 shows the 30.5-MHz ^{15}N CP/MAS NMR spectra of poly(L-leucine), poly(L-phenylalanine) and poly(glycine). The ^{15}N chemical shifts of solid homopolypeptides[47] are

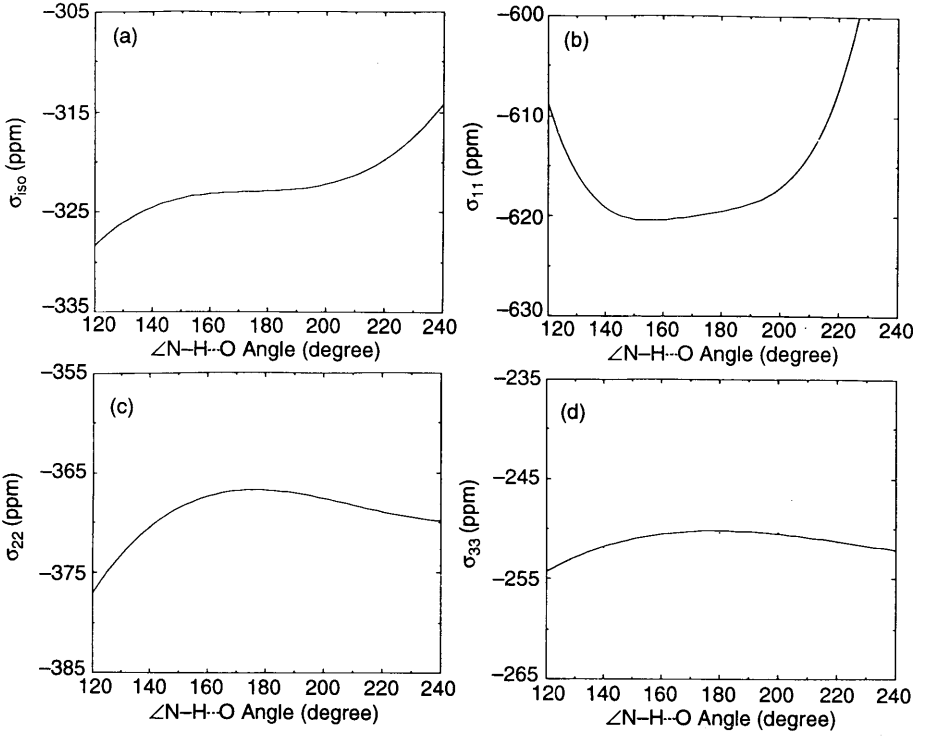

Fig. 15. Variation of the calculated ^{15}N shielding and its tensor components with the hydrogen bond angle (∠N–H···O): (a) σ_{iso}, (b) σ_{11}, (c) σ_{22} and (d) σ_{33}.

summarized in Table 1. Foerster *et al.* suggested that (1) the most interesting observation is the 9–10 ppm low-frequency shift for the right-handed α-helix (α-helix) structures compared to antiparallel β-sheet (β-sheet) structures of poly(L-leucine) and poly(L-phenylalanine), which allows the identification and quantification of the composition of secondary structures of polypeptides; (2) the PGI (β-sheet) and PGII (3_1-helix) forms of poly(glycine) differ by 4.5 ppm in the ^{15}N NMR spectra, whereas the PPI (right-handed 10_3-helix; *cis*-type) and PPII (left-handed 3_1-helix; *trans*-type) of poly(L-proline) do not exhibit any shift differences; (3) all polypeptides having one α-substituent absorb several parts per million to high frequency of poly(glycine) and poly(L-proline) absorbs at the highest frequency; and (4) the shift effects of γ- and δ-carbons are smaller and less systematic in the solid state.

Shoji *et al.*[57] have studied the relation between ^{15}N chemical shift and structural parameters such as primary and secondary structures of various natural abundance homopolypeptides in the solid state. In order to test systematically the power of ^{15}N CP/MAS NMR for the structural analysis of solid polypeptides, they have prepared various kinds of model homopolypeptides:

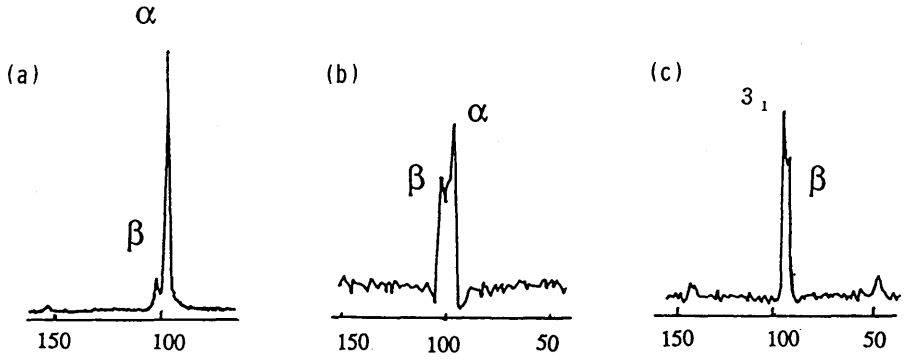

Fig. 16. 30.5-MHz ^{15}N CP/MAS NMR spectra of (a) poly(L-leucine) (d.p. = 50; 10% ^{15}N); (b) poly(L-phenylalanine) (d.p. = 50; 10% ^{15}N; 300 scans); and (c) poly(glycine) (20% ^{15}N; dialyses from LiBr solution; 100 scans).

poly(L-alanine), poly(L-leucine), poly(β-benzyl L-aspartate), poly(γ-benzyl L-glutamate), poly(γ-methyl L-glutamate), poly(L-valine), poly(L-isoleucine), poly(L-glycine) and poly(L-proline), which show characteristic differences in conformation. The 27.4-MHz ^{15}N CP/MAS NMR spectra of natural abundance homopolypeptides, poly(L-alanine) and poly(L-leucine), are shown in Fig. 17. The observed ^{15}N NMR chemical shifts of solid homopolypeptides[57–62]

Table 1. ^{15}N NMR chemical shifts δ (ppm, relative to $^{15}NH_4NO_3$) and linewidths of solid polypeptides.

Polypeptide (d.p.)	Catalyst,[a] solvent, temperature	δ of α-helix structure	δ of sheet structure	Line width (Hz)
Poly(glycine) 50	Benzylamine Acetonitrile/20°C	89.9[b]	85.4	220
Poly(L-alanine) 50	Benzylamine Dioxane/20°C	100.5	—	200
Poly(D,L-alanine) 20	Aniline Dioxane/100°C	—	109.3	300
Poly(L-leucine) 50	Benzylamine Dioxane/20°C	97.9	108.7	150
Poly(D,L-leucine) 50	Benzylamine Dioxane/20°C	98.9	108.5	300
Poly(L-valine) 50	Benzylamine Dioxane/20°C	—	106.9 (105.9)	250
Poly(L-phenylalanine) 50	Isopropylamine Dioxane/20°C	94.7	108.2	—
Poly(γ-methyl-L-glutamate) 50	Benzylamine Dioxane/20°C	97.9	—	200
Poly(L-proline)	Pyridine/20°C	108.8[b]	—	220

[a] Polymerization of amino acid *N*-carboxyanhydrides.
[b] 3_1-Helix.

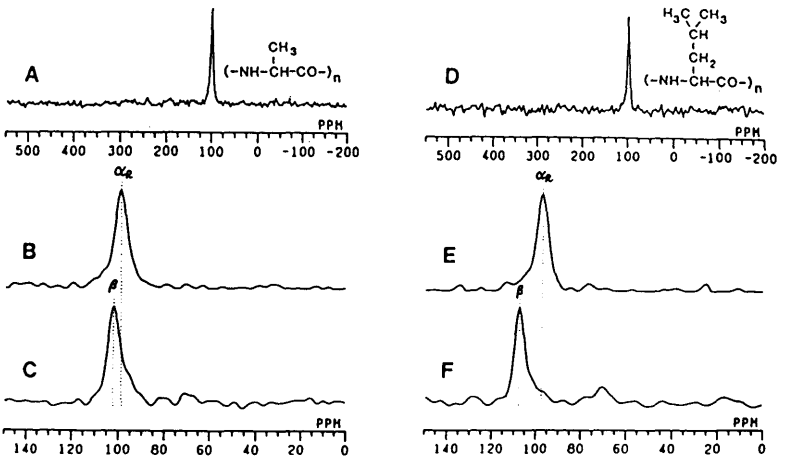

Fig. 17. Natural abundance 27.4-MHz ^{15}N CP/MAS NMR spectra of some poly(L-alanines) and poly(L-leucines) in the solid state. (A and B) PLA1a-50 (α-helix form, 2874 scans); (C) Z-$(Ala)_7$-NHBu (β-sheet form, 1927 scans); (D and E) PLLeu-100 (α-helix, 850 scans); (F) Z-$(Leu)_6$-OEt (β-sheet, 1142 scans).

are summarized in Table 2. It has been confirmed that the isotropic ^{15}N chemical shifts in the peptide backbone of homopolypeptides exhibit a significant conformation-dependent change from the observation and theoretical calculation. It has been found that the σ_{iso} for the α-helix form (97.0–99.2 ppm) appears to low frequency by *ca.* 1.2–10.0 ppm with respect to that for the β-sheet form (99.5–107.0 ppm) of the same homopolypeptides, which obviously depends on the structure of individual amino acid residues. Some ^{15}N chemical shift differences are rather small, but they should be on safe grounds for homopolypeptides. The variations of the σ_{iso} for various kinds of homopolypeptides are *ca.* 2.5 ppm in the α-helix form and *ca.* 7.5 ppm in the β-sheet form. In addition, the σ_{iso} of the β-sheet form of the L-Leu, L-Val, and L-Ile residues, which possess alkyl side-chains, appear to high frequency with respect to that of the L-Ala residue. In contrast, the σ_{iso} value for the β-sheet form of the L-Asp(OBzl), L-Glu(OBzl) and L-Glu(OMe) residues, which possess side-chain esters, is decreased with respect to that of the L-Ala residue. These results indicate that the ^{15}N chemical shift difference between the α-helix and β-sheet forms depends on the side-chain structure of individual amino acid residues.

Another important result is that σ_{iso} gives information about the helix sense (right-handed α-helix or left-handed α-helix) of poly(β-benzyl L-aspartate)[60] (α-helix: 99.2; α_L-helix: 97.0 ppm). In addition, the ^{15}N chemical shift value of PBLAsp-5 (low molecular weight; β-sheet form) is identical with that of PBLAsp-100-III (high molecular weight; β-sheet form), indicating that the ^{15}N chemical shift of a solid polypeptide is independent of the chain length, if no conformational changes occur. Accordingly, the ^{15}N chemical shift depends mainly on the conformation and side-chain structure of individual amino acid

Table 2. Isotropic ^{15}N chemical shifts of some homopolypeptides with various conformations (α-helix, β-sheet, α_L-helix, ω_L-helix, PGI, PGII, PPI and PPII forms) in the solid state (ppm from $^{15}NH_4NO_3$, ±0.5 ppm).

Sample[a]	Conformation[b]	^{15}N δ	Δ δ[c]
PLA1a-50	α-helix	98.6	−3.2
Z-(L-Ala)$_7$-NHBu	β-sheet	101.8	
PLLeu-100	α-helix	97.0	−10.0
Z-(L-Leu)$_6$-OEt	β-sheet	107.0	
PBLAsp-100	α-helix	99.2	−1.2
PBLAsp-100-I	α_L-helix	97.0	
PBLAsp-100-II	ω_L-helix	96.8	
PBLAsp-100-III	β-sheet	100.4	
PBLAsp-5	β-sheet	100.4	
PBLGlu-100	α-helix	97.6	−1.9
Nps-(L-Glu(OBzl))$_6$-NHBu	β-sheet	99.5	
PMLGlu-100	α-helix	97.6	−1.9
Nps-(L-Glu(OMe))$_4$-OH	β-sheet	99.5	
PLVal-100	β-sheet	105.9	
PLIle-100	β-sheet	106.1	
PGly-100	β-sheet (PGI)	83.5	(−5.0)
PGly-100-S	3_1-helix (PGII)	88.5	
PPro-100	10_3-helix (PPI)	107.4	(+2.5)
PPro-100-S	3_1-helix (PPII)	104.9	

[a] Abbreviations: Ala, alanine; Leu, leucine; BLAsp, β-benzyl L-aspartate; BLGlu, γ-benzyl L-glutamate; MLGlu, γ-methyl L-glutamate; Val, valine; Ile, isoleucine; Gly, glycine; Pro, proline; Bu, butyl; Et, ethyl; Bzl, benzyl; Me, methyl; Z, benzyloxycarbonyl; Nps, (*o*-nitrophenyl)sulphenyl.
[b] Abbreviations: PGI, poly(glycine) I form (β-sheet); PGII, poly(glycine) II form (3_1-helix); PPI, poly(L-proline) I form (10_3-helix); PPII, poly(L-proline) II form (3_1-helix).
[c] Differences in the ^{15}N chemical shifts of the α-helix relative to those of the β-sheet form.

residues. Furthermore, Shoji *et al.* have obtained some different results from Forester *et al.*:[47] (1) σ_{iso} of the PGI form of poly(glycine)[61] appears to low frequency by 5 ppm with respect to that of the PGII form, and the PPI and PPII helices of poly(L-proline)[62] differ by 2.5 ppm in the ^{15}N NMR spectra; and (2) the ^{15}N chemical shift of the L-proline residue of $[Pro–Ala–Gly]_n$ (collagen-like triple-helical structure) appears at a higher frequency (108.8 ppm) in comparison with that of poly(L-proline). A diagram of the observed isotropic ^{15}N chemical shift of some homopolypeptides $[X]_n$ with various conformations (α-helix, β-sheet, α_L-helix, ω_L-helix, PGI, PGII, PPI and PPII forms) is shown in Fig. 18.

In order to support the view that ^{15}N chemical shifts are conformation dependent, theoretical calculations of ^{15}N chemical shifts are required, using the electronic states derived by quantum chemical methods. The relative ^{15}N NMR chemical shifts[57] (isotropic magnetic shielding constants) of a dipeptide fragment, *N*-acetyl-L-alanine methylamide (forming hydrogen bonds with two formamide molecules) have been calculated using the FPT-INDO theory,[57,63] as

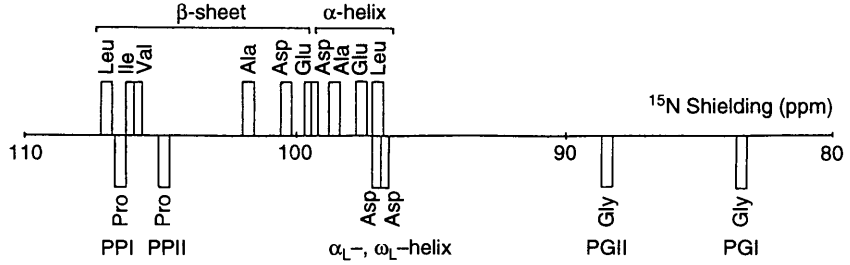

Fig. 18. A diagram of the observed isotropic ^{15}N shielding (σ_{iso}) of some homopolypeptides $[X]_n$ with various conformations (α-helix, β-sheet, α_L-helix, ω_L-helix, PGI, PGII, PPI and PPII forms).

described in Section 3, where the structural data, including the distance between the nitrogen and oxygen atoms, 2.83 and 2.86 Å for the β-sheet and α-helix forms, respectively, were taken from X-ray diffraction studies of poly(L-alanine).[64–66]

Figure 19 shows the observed ^{15}N chemical shift diagram of poly(L-alanine) and the ^{15}N shielding constant (chemical shift) diagram of *N*-acetyl-L-alanine methylamide calculated by the FPT-INDO method. The calculated ^{15}N shieldings for the α-helix and β-sheet forms of poly(L-alanine) are -254.9 and -257.3 ppm, respectively. The calculated ^{15}N chemical shift for the α-helix form appears to low frequency by 2.4 ppm with respect to that of the β-sheet form. This calculated ^{15}N chemical shift displacement is qualitatively in good agreement with the observed one. As a conclusion, the ^{15}N chemical shift of poly(L-alanine) depends on conformation, which can be interpreted mainly in terms of the changes of the electronic structure. Accordingly, ^{15}N chemical shifts determined by the ^{15}N CP/MAS NMR method are very sensitive to the

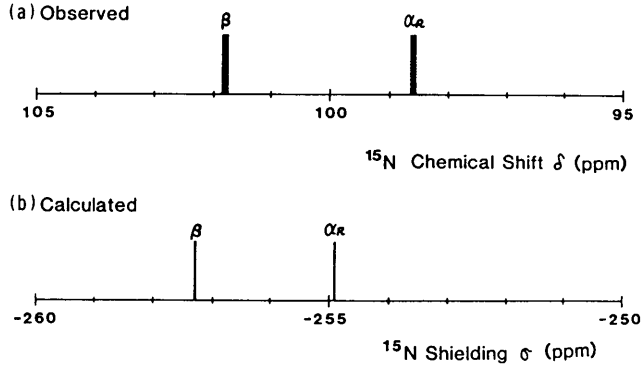

Fig. 19. (a) Observed ^{15}N chemical shift diagram of poly(L-alanine) in the solid state. (b) Calculated ^{15}N shielding diagram of *N*-acetyl-L-alanine methylamide (taking hydrogen bonds with two formamide molecules), as a dipeptide model of poly(L-alanine), by means of the FPT-INDO method.

primary structure such as side-chain effects of a variety of amino acid residues as well as the secondary structure (the main-chain conformation) such as the α-helix and β-sheet forms of homopolypeptides in the solid state.

5.1.2. Copolypeptides

The ^{15}N NMR signals of solid copolypeptides are sensitive to sequence effects; yet they are, in most cases, sensitive to secondary structure. Table 3 shows the ^{15}N chemical shifts of the guest–host copolypeptides in the solid state.[47] It is found that: (1) when a helix-forming amino acid residue such as L-alanine or L-leucine is incorporated into the β-sheet structure of poly(L-valine), the chemical shift has a value typical of the host polypeptide ($\sim$ 108.5 ppm); (2) when the non-helix-forming amino acid residue, L-valine is incorporated into the helices of poly(L-alanine) or poly(L-leucine), it shows the characteristic chemical shift of a helical polypeptide (98.5 $\sim$ 97.5 ppm); (3) glycine incorporated into the α-helix of $[Ala]_n$ does not exhibit any shift difference compared with poly(glycine) in the β-sheet form; (4) when glycine units are incorporated into the β-sheet structures of $[Val]_n$ or $[\beta\text{-Ala}]_n$, they absorb several parts per million to high frequency of the β-sheet of $[Gly]_n$, indicating strong neighbouring sequence effects.

The relation between the isotropic ^{15}N chemical shift and the structural parameters of various kinds of synthetic copolypeptides in the solid state have been studied.[58,59,61,67] For this, a series of ^{15}N-labelled polypeptides were prepared, $[Ala^*, X]_n$, $[Gly^*, X]_n$ and $[Leu^*, X]_n$, consisting of ^{15}N-labelled amino acids (Ala*: L-alanine, Gly*: glycine, Leu*: L-leucine) and other normal amino acids (X; natural abundance of ^{15}N), where the following amino acids were selected for the X residue: (1) L-alanine, D-alanine and L-leucine, which contain

Table 3. ^{15}N NMR chemical shifts δ (ppm, relative to $^{15}NH_4NO_3$) of solid guest–host copolypeptides.

Copolypeptide	Secondary structure	δ of host	δ of guest
Gly* in poly(L-alanine)	α-helix	100.5	85.7
Gly* in poly(γ-methyl-L-glutamate)	α-helix	97.9	87.9
Gly* in poly(L-valine)	β-sheet	105.9	93.4 (90.5–85.1)[a]
Gly* in poly(β-alanine)	β-sheet	99.5	94.4
L-Ala* in poly(L-leucine)	α-helix		99.6
L-Leu* in poly(L-alanine)	α-helix	100.3[a]	97.2
L-Leu* in poly(L-valine)	β-sheet	—	108.5
L-Val* in poly(L-alanine)	α-helix	—	98.5
L-Val* in poly(L-leucine)	α-helix	—	97.5

[a] Poorly resolved shoulders.
* Denotes ^{15}N enrichment.

non-polar hydrocarbon side-chains and stabilize an α-helix; (2) β-benzyl L-aspartate, γ-benzyl L-glutamate, and γ-methyl L-glutamate, which contain polar side-chain esters and stabilize an α-helix; (3) glycine, which is optically inactive and stabilizes a β-sheet; (4) L-valine and L-isoleucine, which contain non-polar hydrocarbon side-chains and stabilize a β-sheet; (5) sarcosine (= *N*-methyl glycine), which destabilizes both an α-helix and a β-sheet.

For the copolypeptides $[Ala^*, X]_n$, the σ_{iso} values of the Ala* residue for the α-helix and β-sheet forms are observed in the range 98.1 $\sim$ 101.5 and 98.8 $\sim$ 107.0 ppm, respectively, as shown in Table 4 and Fig. 20. This suggests that σ_{iso} depends not only on the conformation but also on the primary structure or probably on the higher order structure. Thus, the origin of ^{15}N chemical shifts is rather complex as compared with that of ^{13}C chemical shifts,[68] and it may be generally difficult to estimate the conformation of copolypeptides from the σ_{iso} value. However, σ_{iso} for the α-helix form is always displaced to low frequency with respect to the β-sheet form for the same kind of polypeptide. Another important result is that σ_{iso} gives information about the helix sense of polypeptides by the ^{15}N CP/MAS NMR method. It has been already established by the infrared (IR),[74] far-IR[75] and ^{13}C CP/MAS NMR[68–73] methods that the stable conformation of [Ala*, D-Ala]$_n$ (A3-1 and A3) is the left-handed α-helix; the Ala* residues (minor component, 5 $\sim$ 20 mol%) are incorporated into the left-handed α-helix of the major D-Ala residues. The σ_{iso} values (α_L-helix, 96.5 $\sim$ 96.7 ppm) of the Ala* residues of [Ala*, D-Ala]$_n$ (A3-1 and A3) are displaced to low frequency by *ca.* 2 ppm as compared with that of [L-Ala]$_n$ (α-helix, 98.6 $\sim$ 98.8 ppm, which is exactly equal to σ_{iso} of [D-Ala]$_n$). A similar ^{15}N chemical shift displacement was obtained for the homopolypeptide [L-Asp(OBzl)]$_n$, as described above. Thus, the value of σ_{iso} is sensitive to the helix sense of polypeptides in the solid state.

For the copolypeptides $[Gly^*, X]_n$, the σ_{iso} values of the Gly* residue of the α-helix and β-sheet forms are observed in the ranges 84.2 $\sim$ 85.8 and 83.5 $\sim$ 87.8 ppm, respectively, as shown in Table 5 and Fig. 21. This suggests that the value of σ_{iso} of the Gly* residue depends not only on the conformation but also on the primary structure (or probably on the higher ordered structure). It seems that the displacement of σ_{iso} of the Gly* residue is similar to that of $[Ala^*, X]_n$, and is affected by the strong neighbouring amino acid sequence effects. The origin of ^{15}N chemical shifts is rather complex, and thus it is difficult to directly estimate the conformation of copolypeptides from the σ_{iso} value. The σ_{iso} of the Gly* residue in the α-helix is always displaced to low frequency with respect to the β-sheet form. Furthermore, the σ_{iso} value is displaced to low frequency by 10 $\sim$ 20 ppm with respect to that of homopolypeptides of host amino acid residue [X]$_n$. Thus, it is emphasized that σ_{iso} may be useful for the study on such a conformational change of copolypeptides having identical primary structure and some natural proteins such as collagen fibrils or silk fibroins.

In contrast, for the copolypeptides $[Leu^*, X]_n$ (except for $[Leu^*, Gly]_n$ in the

Table 4. Isotropic ^{15}N shielding (σ_{iso}), ^{15}N principal shielding elements ($\sigma_{11}, \sigma_{22}, \sigma_{33}$), anisotropy ($\Delta\sigma$) and asymmetry parameter (η) of solid polypeptides $[Ala^*, X]_n$ containing ^{15}N-labelled L-alanine residue in the α-helix, α_L-helix, and β-sheet forms.

	Sample	Composition[a] (%)			Conformation[b]	^{15}N shielding[c] (ppm)				$\Delta\sigma$[d]	η[e]
		Ala*	Ala	X		σ_{iso}	σ_{11}	σ_{22}	σ_{33}		
A1	$[Ala^*]_n$	20	80		α-helix	98.8	204	54.4	38	158	0.16
A2	$[Ala^*]_n$-5	20	80		β-sheet	102.2	201	61.7	44	148	0.18
A3-1	$[Ala^*, D\text{-}Ala]_n$	5	0	95	α_L-helix	96.7	197	57.1	36	151	0.21
A3	$[Ala^*, D\text{-}Ala]_n$	20	0	80	α_L-helix	96.5	198	55.1	36	153	0.19
A4	$[Ala^*, Gly]_n$	20	0	80	β-sheet	98.8	200	59.6	37	152	0.22
A5	$[Ala^*, Gly]_n$	20	60	20	α-helix	98.6	202	57.4	36	155	0.21
A6-1	$[Ala^*, Leu]_n$	5	0	95	α-helix	98.6	205	56.0	35	160	0.20
A6	$[Ala^*, Leu]_n$	20	0	80	α-helix	98.6	204	56.9	35	158	0.21
A6-2	$[Ala^*, Leu]_n$	5	45	50	α-helix	98.3	207	54.2	34	163	0.19
A6-3	$[Ala^*, Leu]_n$	5	75	20	α-helix	98.1	203	57.1	34	158	0.22
A7-1	$[Ala^*, Val]_n$	5	0	95	β-sheet	107.0	210	63.5	47	155	0.16
A7	$[Ala^*, Val]_n$	20	0	80	β-sheet[f]	99.7	202	62.4	35	153	0.27
A7-2	$[Ala^*, Val]_n$	5	25	70	α-helix[g]	98.6	201	53.1	42	154	0.11
A8	$[Ala^*, Ile]_n$	20	0	80	β-sheet	101.0	200	63.0	40	149	0.23
A9-1	$[Ala^*, Asp(OBzl)]_n$	5	0	95	α-helix	101.3	210	54.7	39	163	0.14
A9-2	$[Ala^*, Asp(OBzl)]_n$	10	0	90	α-helix	101.1	210	56.0	37	164	0.17
A9	$[Ala^*, Asp(OBzl)]_n$	20	0	80	α-helix	101.5	208	58.7	38	160	0.19
A10	$[Ala^*, Glu(OBzl)]_n$	20	0	80	α-helix	100.4	206	56.7	39	158	0.17
A11	$[Ala^*, Glu(OMe)]_n$	20	0	80	α-helix[h]	99.9	205	58.1	37	157	0.20
A12	$[Ala^*, Sar]_n$	20	0	80	?	99.0	198	62.2	37	148	0.26

[a] Copolymer composition (%). Abbreviations: Ala*, ^{15}N-labelled L-alanine (99 atom % of ^{15}N purity); Ala, L-alanine (natural abundance of ^{15}N); X, other amino acids (natural abundance of ^{15}N).

[b] Abbreviations: α-helix, right-handed α-helix; α_L-helix, left-handed α-helix; β-sheet, antiparallel β-sheet.

[c] ^{15}N shielding of Ala* of polypeptides: ± 0.5 ppm for σ_{iso} and σ_{22} and ± 2 ppm for σ_{11} and σ_{33}, from $^{15}NH_4NO_3$.

[d] Anisotropy: $\Delta\sigma = \sigma_{11} - (\sigma_{22} + \sigma_{33})/2$.

[e] Asymmetry parameter: $\eta = (\sigma_{22} - \sigma_{33})/(\sigma_{11} - \sigma_{iso})$.

[f] Major conformation of $[Ala^*, Val]_n$ (A7) is the β-sheet form containing small amounts (assumed below 10–20%) of the α-helix form.

[g] Major conformation of $[Ala^*, Val]_n$ (A7-2) is the α-helix form containing small amounts (assumed below 10%) of the β-sheet form.

[h] Major conformation of $[Ala^*, Glu(OMe)]_n$ is the α-helix form containing small amounts (assumed below 20–30%) of the β-sheet form.

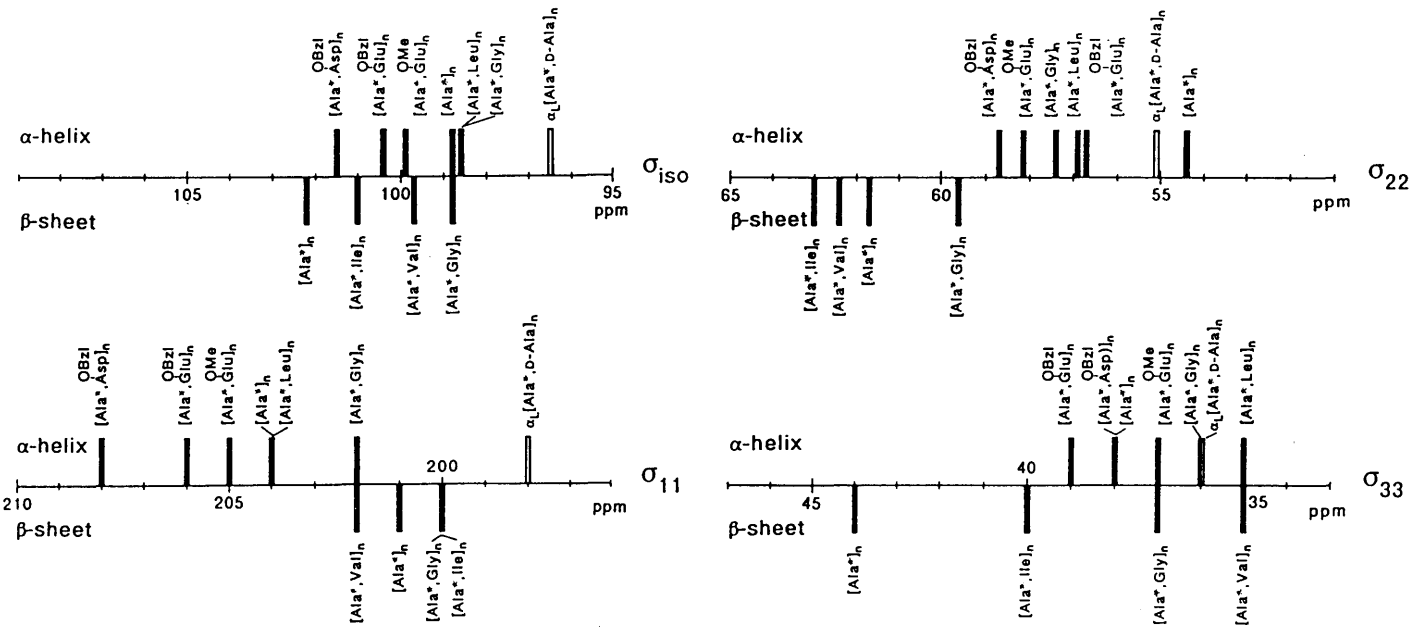

Fig. 20. A diagram of the observed isotropic ^{15}N shielding (σ_{iso}) and the principal shielding elements (σ_{11}, σ_{22} and σ_{33}) of the Ala* residue of some polypeptides [Ala*, X]$_n$ (Ala* content is nearly 20%) in the solid state.

Table 5. Isotropic ^{15}N shieldings (σ_{iso}), ^{15}N principal shielding elements ($\sigma_{11}, \sigma_{22}, \sigma_{33}$), anisotropy ($\Delta\sigma$) and asymmetry parameter (η) of solid polypeptides $[Gly^*, X]_n$ containing ^{15}N-labelled glycine residue.

	Sample	Composition[a] (%)			Conformation[b]	^{15}N shielding[c] (ppm)				$\Delta\sigma$[d]	η[e]
		Gly*	Gly	X		σ_{iso}	σ_{11}	σ_{22}	σ_{33}		
G1	$[Gly^*]_n$	20	80		β-sheet	83.5	185	40.7	25	152	0.15
G1-S	$[Gly^*]_n$	20	80		3_1-helix	88.5	194	42.1	29	158	0.12
G2	$[Gly^*, Ala]_n$	20	0	80	α-helix	84.2	192	36.9	24	162	0.12
G3	$[Gly^*, Ala]_n$	20	60	20	β-sheet	83.5	186	45.3	19	154	0.26
G4-1	$[Gly^*, Leu]_n$	5	0	95	α-helix	84.5	190	38.7	25	158	0.13
G4-2	$[Gly^*, Leu]_n$	5	5	90	α-helix	84.4	190	38.9	24	159	0.14
G4	$[Gly^*, Leu]_n$	20	0	80	α-helix	85.3	190	41.0	25	157	0.15
G4-3	$[Gly^*, Leu]_n$	5	45	50	α-helix	84.4	186	43.0	24	153	0.19
G4-4	$[Gly^*, Leu]_n$	20	60	20	β-sheet	83.7	186	45.5	20	153	0.25
G5	$[Gly^*, Val]_n$	20	0	80	β-sheet	85.1	183	53.9	19	147	0.36
G6	$[Gly^*, Ile]_n$	20	0	80	β-sheet	87.8	189	47.6	25	153	0.22
G7	$[Gly^*, Asp(OBzl)]_n$	20	0	80	α-helix	86.0	188	50.8	19	153	0.31
G8	$[Gly^*, Glu(OBzl)]_n$	20	0	80	α-helix	85.8	190	40.5	27	156	0.13

[a] Copolymer composition (%). Abbreviations: Gly*, ^{15}N-labelled glycine (99 atom % of ^{15}N purity); Gly, glycine (natural abundance of ^{15}N); X, other amino acids (natural abundance of ^{15}N).

[b] Abbreviations: α-helix, right-handed α-helix; β-sheet, antiparallel β-sheet; PGI, polyglycine I form; PGII, polyglycine II form.

[c] ^{15}N shielding of Gly* of polypeptides (from $^{15}NH_4NO_3$).

[d] Anisotropy.

[e] Asymmetry parameter.

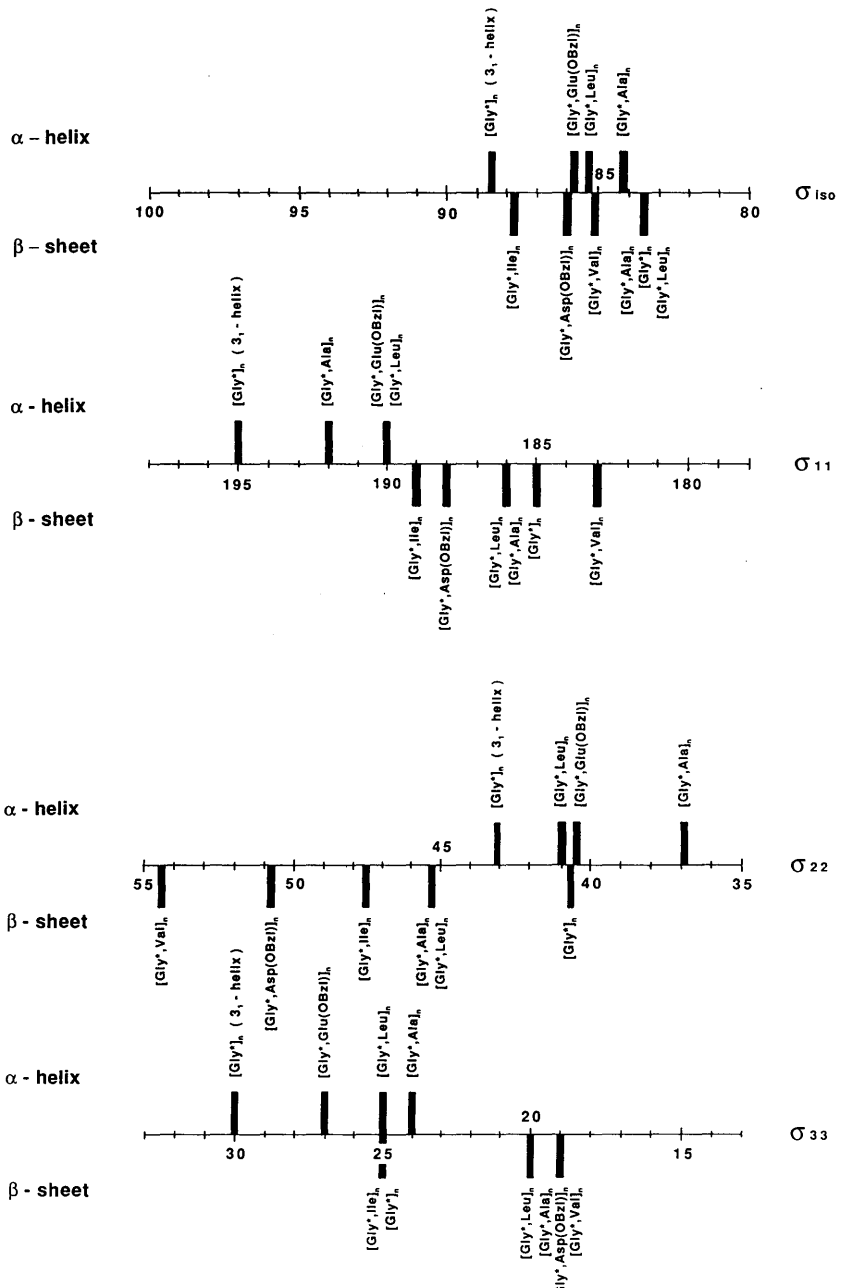

Fig. 21. A diagram of the observed isotropic ^{15}N shielding (σ_{iso}) and the principal shielding elements (σ_{11}, σ_{22} and σ_{33}) of the Gly* residue of some polypeptides [Gly*, X]$_n$ (Gly* content is nearly 20%) in the solid state.

β-sheet form), the σ_{iso} values of the Leu* residue of the α-helix and β-sheet forms are observed in the ranges 96.2 $\sim$ 97.7 and 105.1 $\sim$ 107.0 ppm, respectively, as shown in Table 6 and Fig. 22. The σ_{iso} values are very similar to those of the homopolypeptide $[Leu^*]_n$ (α-helix: 97.0 and β-sheet: 107.0 ppm). It is noteworthy that the ^{15}N chemical shift difference of the Leu* residue between the α-helix and the β-sheet forms is large (7–11 ppm), but that the ^{15}N chemical shift differences from the neighbouring amino acid sequence effects are small (within 2 ppm). This is quite a different result from those obtained for $[Ala^*, X]_n$ and $[Gly^*, X]_n$. Thus, the origin of ^{15}N chemical shifts of the Leu* residue is rather simple compared with that of the Ala* or Gly* residues. Since the σ_{iso} value of the Leu* residue depends mainly on the conformation, with a very small dependence on the primary structure (or higher ordered structure), it may be very useful for the conformational analysis of copolypeptides in the solid state.

As mentioned above, it has been shown that the origin of the isotropic

Table 6. Isotropic ^{15}N shielding (σ_{iso}) and ^{15}N shielding tensor element (σ_{22}) of solid polypeptides $[Leu^*, X]_n$ containing ^{15}N-labelled L-leucine residue in the α-helix and β-sheet forms.

	Sample	Composition[a] (%)			Conformation	^{15}N shielding[b] (ppm)	
		Leu*	Leu	X		σ_{iso}	σ_{22}
L1	$[Leu^*]_n$	20	80		α-helix	97.0	55.7
L2	$[Leu^*]_n$-5	20	80		β-sheet	107.0	66.9
L3	$[Leu^*, Val]_n$	20	0	80	β-sheet	107.0	65.1
L3-1	$[Leu^*, Val]_n$	20	10	70	β-sheet[c]	107.0 (97.0)	65.3
L3-2	$[Leu^*, Val]_n$	20	30	50	α-helix	97.0	55.3
L3-3	$[Leu^*, Val]_n$	20	50	30	α-helix	96.9	54.0
L3-4	$[Leu^*, Val]_n$	20	60	20	α-helix	96.8	54.0
L4	$[Leu^*, Ala]_n$	20	0	80	α-helix	96.2	55.5
L4-1	$[Leu^*, Ala]_n$	20	30	50	α-helix	96.5	55.5
L4-2	$[Leu^*, Ala]_n$	20	60	20	α-helix	96.8	51.0
L5	$[Leu^*, Gly]_n$	20	0	80	β-sheet	96.9	61.2
L5-1	$[Leu^*, Gly]_n$	20	30	50	α-helix	97.2	55.5
L5-2	$[Leu^*, Gly]_n$	20	60	20	α-helix	96.8	53.2
L6	$[Leu^*, Lys(Z)]_n$	20	0	80	β-sheet[d]	105.1 (97.2)	63.0
L7	$[Leu^*, Ile]_n$	20	0	80	β-sheet	106.7	58.0
L7-1	$[Leu^*, Ile]_n$	20	30	50	α-helix	97.1	56.0
L8	$[Leu^*, Asp(OBzl)]_n$	20	30	50	α-helix	97.7	56.7
L9	$[Leu^*, Glu(OBzl)]_n$	20	30	50	α-helix	97.6	50.1

[a] Copolymer composition (%): Leu*, ^{15}N-labelled L-leucine (99 atom % of ^{15}N purity).
[b] ^{15}N shielding of Leu* of polypeptides (±0.5 ppm, from $^{15}NH_4NO_3$).
[c] Major conformation of $[Leu^*, Val]_n$ (L3-1) is the β-sheet form containing small amounts (assumed below 30–40%) of the α-helix form.
[d] Major conformation of $[Leu^*, Lys(Z)]_n$ (L6) is the β-sheet form containing small amounts (assumed below 25–35%) of the α-helix form.

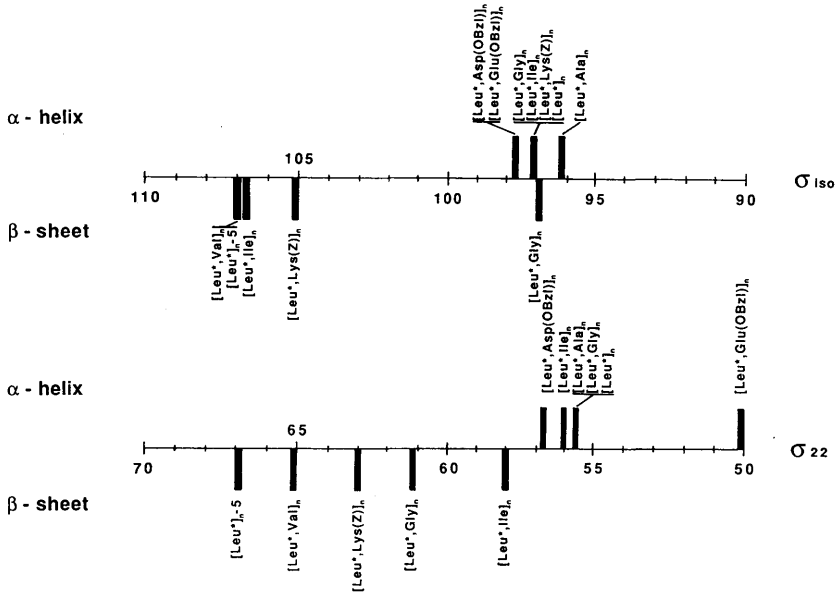

Fig. 22. A diagram of the observed isotropic ^{15}N shielding (σ_{iso}) and the principal shielding element (σ_{22}) of the Leu* residue of some polypeptides $[Leu^*, X]_n$ (Leu* content is nearly 20%) in the solid state.

^{15}N chemical shifts of copolypeptides is related to the conformation, the side-chain effects of amino acid residue and neighbouring amino acid sequence effects.[58–62,67] Especially, for the Leu* residue, the σ_{iso} value depends mainly on conformation, and the neighbouring amino acid sequence effects are very small. In contrast, for the Ala* and Gly* residues, the σ_{iso} value depends both on conformation and strong neighbouring amino acid sequence effects.

In α-helical copolypeptides $[Leu^*, X]_n$ such as $[Leu^*, Ala]_n$, [Leu*, Glu(OBzl)]$_n$, and [Leu*, Asp(OBzl)]$_n$, the σ_{iso} values of the Leu* are displaced to low frequency by $0 \sim 2.5$ ppm with respect to those of the corresponding host homopolypeptide $[X]_n$. In β-sheet copolypeptides such as $[Leu^*, Val]_n$ and $[Leu^*, Ile]_n$, the σ_{iso} values are displaced to high frequency by $0.6 \sim 1.1$ ppm with respect to those of the corresponding host homopolypeptide. As a result, the σ_{iso} regions of the Leu* for the $[Leu^*, X]_n$ with the α-helix ($96 \sim 98$ ppm) and β-sheet forms ($106 \sim 107$ ppm) are distinguishable. That is to say, the σ_{iso} value of the Leu* residues depends mainly upon the conformation of the copolypeptides in the solid state.

In α-helical copolypeptides $[Ala^*, X]_n$ such as $[Ala^*, Leu]_n$, [Ala*, Asp(OBzl)]$_n$, [Ala*, Glu(OBzl)]$_n$ and [Ala*, Glu(OMe)]$_n$, the σ_{iso} values of the Ala* are displaced conversely to high frequency by $2 \sim 3$ ppm with respect to those of the corresponding host homopolypeptide $[X]_n$ (see Fig. 23). In β-sheet

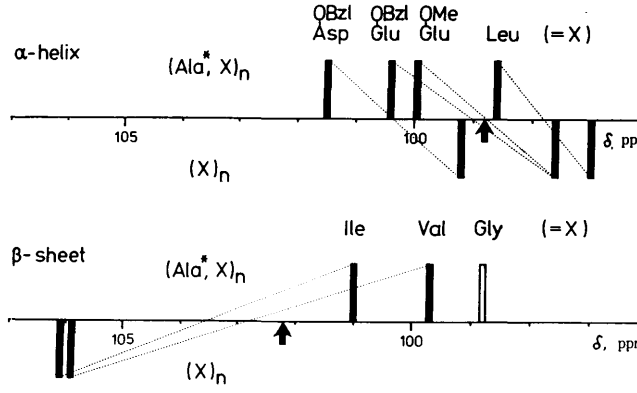

Fig. 23. Correlation of the ^{15}N chemical shifts of Ala* of copolypeptides, $[Ala^*, X]_n$, with those of host homopolypeptides $[X]_n$ in the solid state. The arrow indicates the ^{15}N chemical shift of poly(L-alanine).

copolypeptides such as $[Ala^*, Val]_n$ and $[Ala^*, Ile]_n$, the σ_{iso} values of the Ala* are displaced to low frequency by 5–6 ppm with respect to those of the corresponding host homopolypeptide. For this, the σ_{iso} regions of the Ala* in the copolypeptides with the α-helix (98 ~ 102 ppm) and β-sheet forms (99 ~ 102 ppm) are overlapping.

Furthermore, in α-helical copolypeptides $[Gly^*, X]_n$ such as $[Gly^*, Ala]_n$, $[Gly^*, Leu]_n$, $[Gly^*, Glu(OBzl)]_n$ and $[Gly^*, Asp(OBzl)]_n$, the σ_{iso} values of the Gly* are displaced to low frequency by 12 ~ 15 ppm with respect to those of the corresponding host homopolypeptide $[X]_n$ (see Fig. 24). In β-sheet copolypeptides such as $[Gly^*, Ala]_n$, $[Gly^*, Leu]_n$, $[Gly^*, Val]_n$, $[Gly^*, Ile]_n$, and $[Gly^*, Asp(OBzl)]_n$, the σ_{iso} values of the Gly* are displaced to low frequency

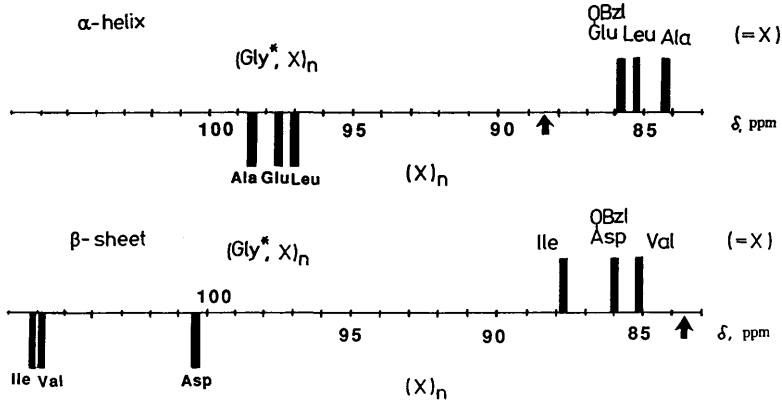

Fig. 24. Correlation of the ^{15}N chemical shifts of Gly* of copolypeptides, $[Gly^*, X]_n$, with those of host homopolypeptides $[X]_n$ in the solid state. The arrow indicates the ^{15}N chemical shift of poly(glycine).

by $14 \sim 22$ ppm with respect to that of the corresponding host homopolypeptide. As a result, the σ_{iso} regions of the Gly* in the copolypeptides with the α-helix ($84 \sim 86$ ppm) and β-sheet forms ($83 \sim 88$ ppm) are overlapping. It is very interesting that the σ_{iso} values of copolypeptides depend on side-chain effects of amino acid residues. Especially for the Ala* and Gly* residues, the σ_{iso} values depend on strong neighbouring amino acid sequence effects. Although the origin of ^{15}N chemical shifts is rather complex, this point needs further clarification.

The relationship between the σ_{iso} value and the copolymer composition for copolypeptides has been studied. Figures 25 and 26 show the plots of the σ_{iso} data of the Ala* residue in $[Ala^*, Leu]_n$ and $[Ala^*, Val]_n$, respectively, against the L-alanine content (%). For a series of $[Ala^*, Leu]_n$, where Leu has a hydrophobic alkyl side-chain and stabilizes an α-helix conformation, σ_{iso} is found to be almost constant over a wide range of L-alanine contents ($5 \sim 80\%$).

In contrast, for a series of $[Ala^*, Val]_n$, where the Val residue has a hydrophobic side-chain and stabilizes a β-sheet form, the stable conformation was found to be the β-sheet form at $\leq 20\%$ L-alanine content (A7-1, A7) and α-helix form at $\geq 30\%$ L-alanine content (A7-2). In this narrow range of

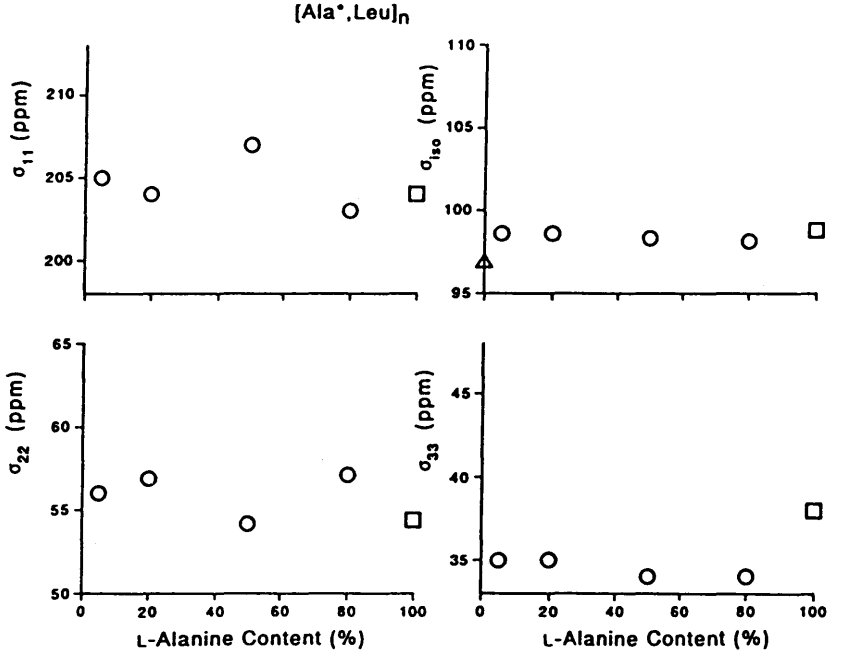

Fig. 25. Plots of the isotropic ^{15}N shielding (σ_{iso}) and the principal shielding elements (σ_{11}, σ_{22} and σ_{33}) of the Ala* residue in $[Ala^*, Leu]_n$ against the L-alanine content (%): (○) α-helix form; (□) poly(L-alanine) (α-helix form); (△) poly(L-leucine) (α-helix form).

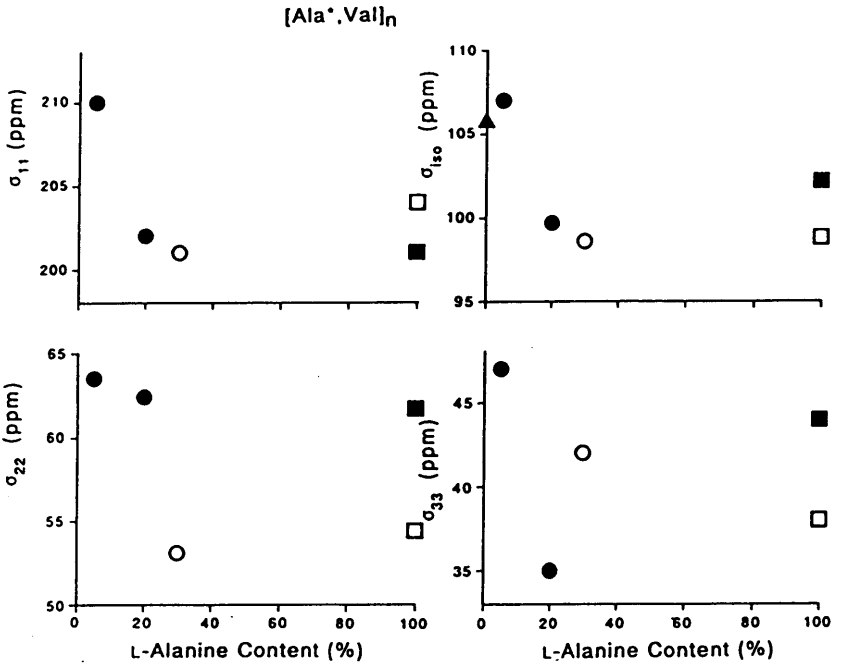

Fig. 26. Plots of the isotropic ^{15}N shielding (σ_{iso}) and the principal shielding elements (σ_{11}, σ_{22} and σ_{33}) of the Ala* residue in [Ala*, Val]$_n$ against the L-alanine content (%): (○) α-helix form; (●) β-sheet form; (□) poly(L-alanine) (α-helix form); (■) poly-(L-alanine) (β-sheet form); (▲) poly(L-valine) (β-sheet form).

L-alanine content (between 20 and 30%), any significant changes in σ_{iso} are not observed. A large chemical shift change was observed for σ_{iso} at $5 \sim 20\%$ L-alanine content. Such chemical shift changes may be mainly due to the side-chain effect of the L-valine residue and the neighbouring amino acid sequence effects, but apparently are not due to the main-chain conformation of copolypeptides.

Figures 27 and 28 show the plots of the σ_{iso} value of the Gly* residue in [Gly*, Ala]$_n$ and [Gly*, Leu]$_n$, respectively, against the glycine content.

For a series of [Gly*, Ala]$_n$ and [Gly*, Leu]$_n$, σ_{iso} is almost constant, indicating that this is independent of the wide range of L-alanine contents ($5 \sim 80\%$). Accordingly, for a series of [Gly*, Ala]$_n$ and [Gly*, Leu]$_n$, the chemical shift displacements in σ_{iso} may be indepenent of the main-chain conformation of copolypeptides. The reason for this is not clarified yet.

Figure 29 shows the plots of σ_{iso} of the Leu* residue in [Leu*, Ala]$_n$, [Leu*, Gly]$_n$ and [Ala*, Val]$_n$, respectively, against the L-leucine content (%). For all of the series of [Leu*, Ala]$_n$, [Leu*, Gly]$_n$, , [Leu*, Val]$_n$, the changes of the values of σ_{iso} are negligibly small against copolymer

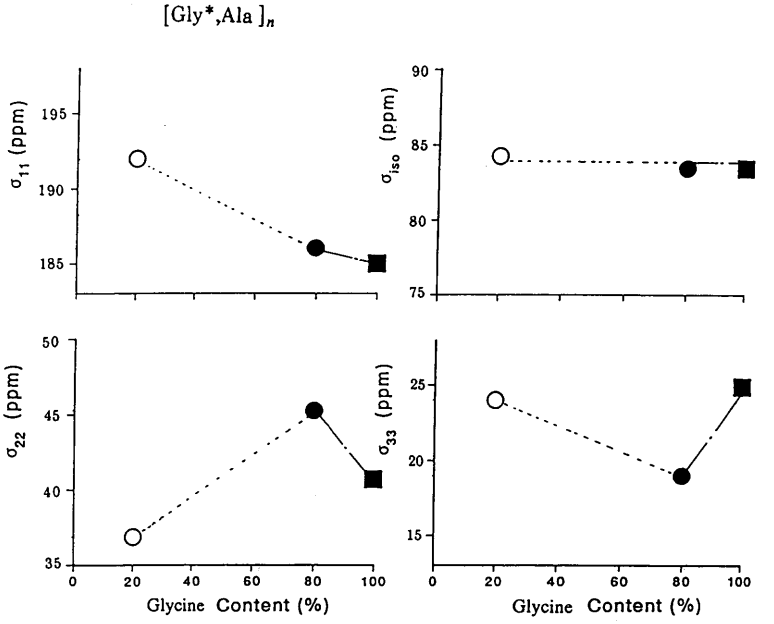

Fig. 27. Plots of the isotropic ^{15}N shielding (σ_{iso}) and the principal shielding elements (σ_{11}, σ_{22} and σ_{33}) of the Gly* residue in [Gly*, Ala]$_n$ against the glycine content (%): (○) α-helix form; (●) β-sheet form; (■) poly(glycine) (β-sheet form).

composition, where no conformational changes occur. In contrast, a large chemical shift displacement (*ca.* 8 ~ 10 ppm) was observed between the α-helix and β-sheet forms, which is ascribed to the main-chain conformation of copolypeptides.

5.2. Principal values of ^{15}N shielding tensors (σ_{11}, σ_{22} and σ_{33})

The development of high-resolution solid-state NMR techniques has made possible the study of shielding tensors. No doubt ^{15}N will receive more attention in the near future for a number of reasons such as the increased availability of high-field spectrometers and the development of polarization transfer techniques for solids. Recently some interesting results on the relation between ^{15}N shielding tensors and structures of solid polypeptides have been reported. Nitrogen NMR could, therefore, be a useful intrinsic probe in ^{15}N NMR studies of polypeptides and proteins in the solid state, particularly in cases where selective ^{15}N labelling is possible.

5.2.1. Homopolypeptides

The principal values of the ^{15}N shielding tensors were obtained by fitting the

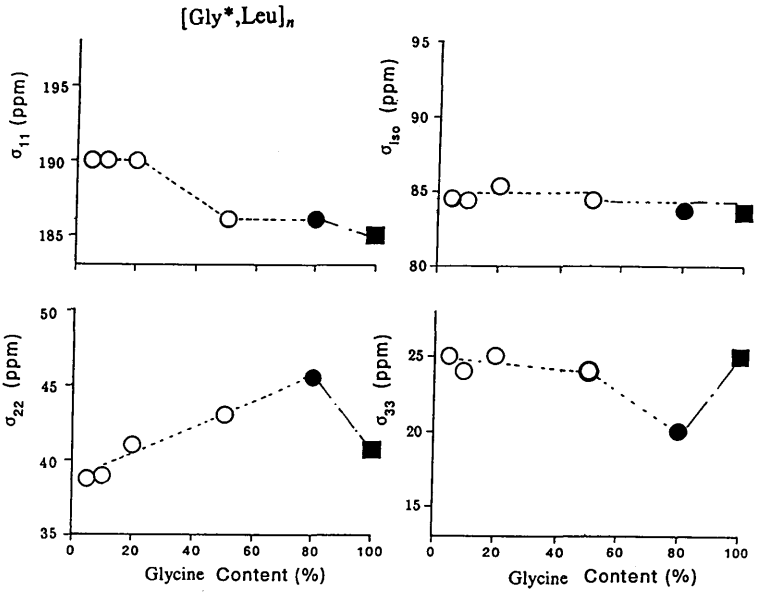

Fig. 28. Plots of the isotropic ^{15}N shielding (σ_{iso}) and the principal shielding elements (σ_{11}, σ_{22} and σ_{33}) of the Gly* residue in [Gly*, Leu]$_n$ against the glycine content (%): (○) α-helix form; (●) β-sheet form; (■) poly(glycine) (β-sheet form).

theoretical powder pattern lineshape[58] which is convoluted with Lorentzian functions to the observed powder patterns (Fig. 30). The σ_{iso} and σ_{22} data can be read directly from the observed CP/MAS and powder pattern (CP-static) spectra, respectively. The error limits of the σ_{11} and σ_{33} values ($\leq \pm 2$ ppm) are larger than those for σ_{iso} and σ_{22} ($\leq \pm 0.5$ ppm).[58,59]

Table 4 summarizes the isotropic ^{15}N shielding (σ_{iso}) and principal values of the ^{15}N shielding tensors of [Ala*]$_n$ and [Ala*, X]$_n$. The σ_{11}, σ_{22}, and σ_{33} data of the α-helical [Ala*]$_n$ are decreased by −3, 7.3, and 6 ppm, respectively, with respect to the β-sheet [Ala*]$_n$ in the solid state. For [Ala*]$_n$, (1) only the σ_{11} value of the α-helix form appears to high frequency with respect to that of the β-sheet form, whereas the other values (σ_{22} and σ_{33}) of the α-helix appear to low frequency with respect to those of the β-sheet and (2) the differences between the σ_{22} (and σ_{33}) values for the α-helix and β-sheet forms are larger than those of σ_{iso}.

On the other hand, the σ_{11}, σ_{22} and σ_{33} values of the α-helical [Leu*]$_n$ are decreased by 5, 11.2 and 2 ppm, respectively, with respect to those of the β-sheet [Leu*]$_n$ in the solid state (Table 6). The displacement of the σ_{11}, σ_{22} and σ_{33} values between the α-helical [Leu*]$_n$ and the β-sheet [Leu*]$_n$ is different from those of the [Ala*]$_n$, the reason for which is unclear at present. For [Leu*]$_n$, (1) all principal values of the nitrogen shielding tensor of α-helical

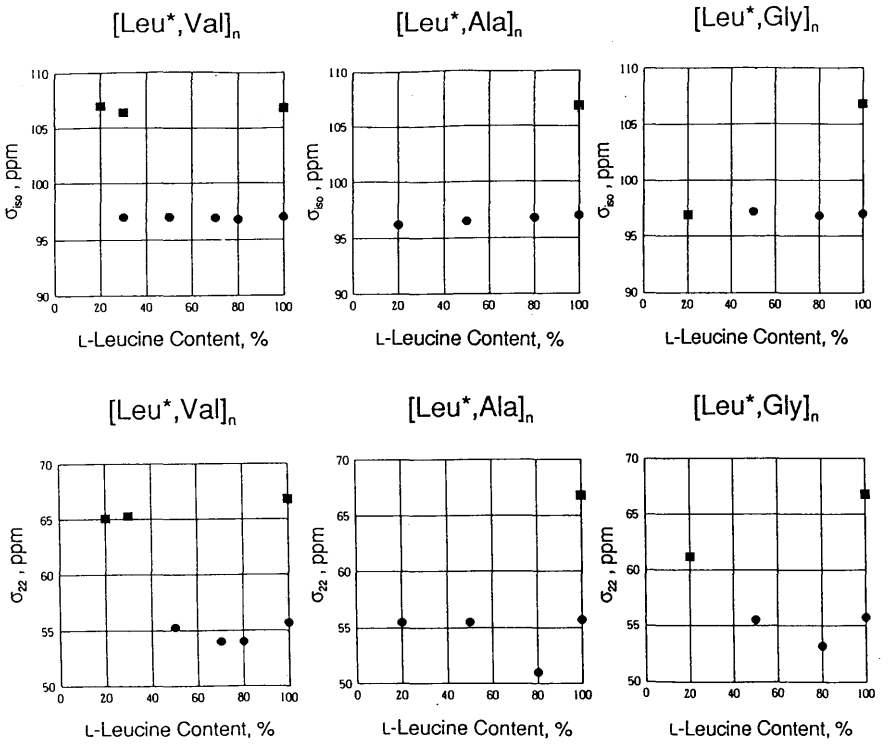

Fig. 29. Plots of the isotropic ^{15}N shielding (σ_{iso}) and the principal shielding element (σ_{22}) of the Leu* residue in [Leu*, Val]$_n$, [Leu*, Ala]$_n$ and [Leu*, Gly]$_n$ against the L-leucine content (%): (●) α-helix form; (■) (β-sheet form).

[Leu*]$_n$ are displaced to low frequency with respect to those of the β-sheet one and (2) the difference between the σ_{22} values of these two forms is quite large with respect to those of the others (σ_{11} and σ_{33}).

Next, the σ_{11}, σ_{22} and σ_{33} values of the PGII form are displaced to high frequency by 9, 1.4 and 4 ppm, respectively, with respect to those of the PGI form (Table 5). For [Gly*]$_n$, (1) all of principal values of the PGII form are displaced to high frequency with respect to those of the β-sheet form and (2) the difference between the σ_{11} values of these two forms is large with respect to those of the others (σ_{22} and σ_{33}).

Why is the displacement of the σ_{11} different for [Ala*]$_n$ and [Leu*]$_n$? The reason for this is not clear at present, but this is a very important question in reaching and understanding of the correlation between structures and the ^{15}N shielding tensor. The ^{15}N shielding tensor may be useful for conformational analysis of solid polypeptides, if the origin of the chemical shift displacements can be elucidated.

According to recent work by Oas *et al.*[36,37] the alignment of the ^{15}N shielding tensors of L-[1-^{13}C]-alanyl-L-[^{15}N]-alanine has been determined from the

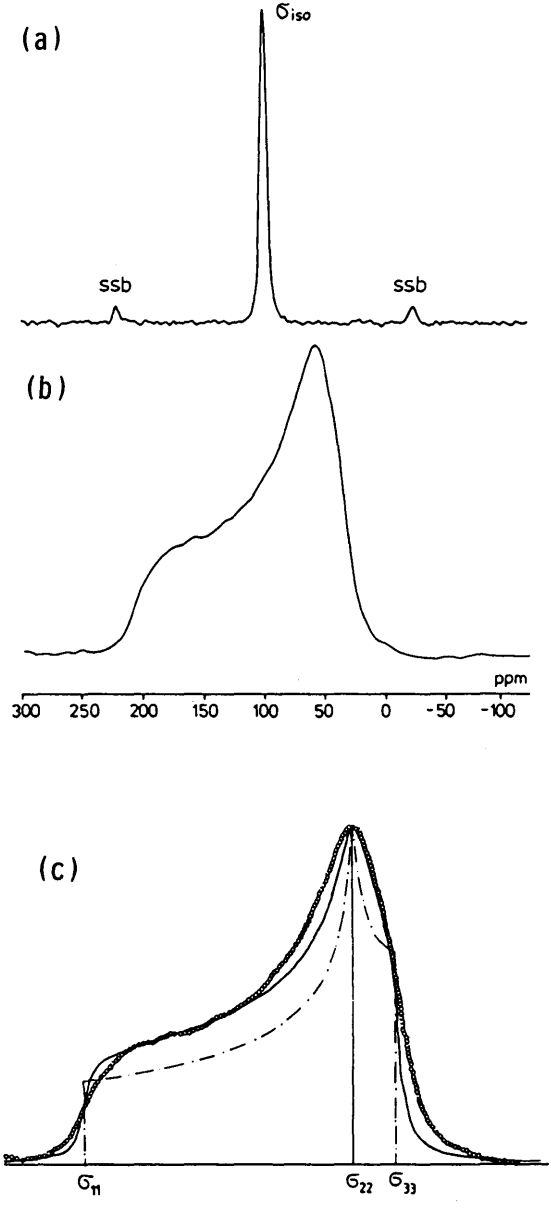

Fig. 30. 27.4-MHz ^{15}N CP/MAS NMR spectra (a), ^{15}N CP-static (powder pattern) NMR spectra (b), and theoretical powder pattern (– · –) (c) (convoluted with the Lorentzian function (——) and experimental points (○)) for $[Ala^*, Leu]_n$ (A-6).

dipole-coupled powder patterns. It was assumed that the orientations of σ_{11} (nearly parallel to the N–H bond) and σ_{33} (parallel to the C′–N bond) lie in the peptide plane but that the orientation of σ_{22} is perpendicular to the peptide bond (Fig. 31). It has been accepted that the alignment of the tensor element σ_{11} is nearly parallel to the hydrogen bonding (N–H $\cdots$ O) direction,[34,36,37] whereas the alignments of σ_{22} and σ_{33} are not always decided. Therefore, σ_{11} may offer certain information about the manner of the hydrogen bonding of polypeptides and proteins.

5.2.2. Copolypeptides

Figure 20 shows the diagram of the observed ^{15}N data of the Ala* residue of some polypeptides $[Ala^*, X]_n$ (Ala* content is nearly 20%). The range of σ_{22} values of the α-helical $[Ala^*, X]_n$ is displaced to low frequency with respect to those of the β-sheet $[Ala^*, X]_n$, whereas the range of σ_{11} values of the α-helix is displaced to high frequency with respect to that of the β-sheet form. The dependence of the displacement of σ_{33} on conformation is ambiguous for $[Ala^*, X]_n$. This result is consistent with that of $[Ala^*]_n$. Since the alignment of the tensor element σ_{11} is nearly parallel to the hydrogen-bonding (N–H $\cdots$ O) direction,[32,34,36,37] it is anticipated that σ_{11} may offer certain information about the manner of the hydrogen bonding of polypeptides. In addition, the σ_{11} of the Ala* residues of $[Ala^*, \text{D-Ala}]_n$ (A3, α_L-helix) is significantly decreased by 6 ppm with respect to that of $[Ala^*]_n$ (A1, α-helix), whereas the difference between the right-handed and left-handed α-helices is not so large for σ_{22} (0.7 ppm) and σ_{33} (2 ppm). This indicates that σ_{11} is sensitive to the helical sense as well as the manner of the hydrogen bonding.

The displacement of σ_{22} of $[Ala^*, X]_n$ is very sensitive to the conformational changes of copolypeptides. The σ_{22} values of the Ala* of the α-helix and β-sheet forms are observed separately in the ranges $54 \sim 59$ and $61 \sim 63$ ppm, respectively. The variation of the values of σ_{11}, σ_{22} and σ_{33} among the α-helical $[Ala^*, X]_n$ is 6, 4.3 and 4 ppm, respectively. The variation of the values of σ_{11}, σ_{22} and σ_{33} among the β-sheet $[Ala^*, X]_n$ is 2, 3.4 and 9 ppm. The variation of the σ_{33} data among the β-sheet form is very large with respect to that of the α-helix form. This suggests that σ_{33} may be related to side-chain structures of copolypeptides.

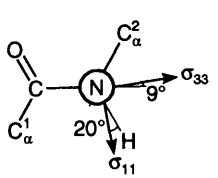

Fig. 31. The orientation of σ_{11}, σ_{22} and σ_{33} of a peptide: the orientation of σ_{11} and σ_{33} in the peptide plane, assuming σ_{22} is perpendicular to the peptide plane and positive above the page. (From Ref. 36.)

Figures 25 and 26 show the plots of σ_{iso}, σ_{11}, σ_{22}, and σ_{33} of various [Ala*, Leu]$_n$, and [Ala*, Val]$_n$, respectively, against the L-alanine content. The changes of σ_{iso} and σ_{33} are negligibly small over a wide range of L-alanine content ($5 \sim 80\%$). In contrast, the σ_{11} and σ_{22} data seem to depend slightly on the L-alanine content: σ_{22} value at 50% L-alanine content seems to be displaced to low frequency, whereas the σ_{11} value at 50% L-alanine content seems to be displaced to high frequency with respect to that of other contents. The reason for this is not clarified yet.

For a series of [Ala*, Asp(OBzl)]$_n$, the value of σ_{22} decreases linearly as the L-alanine content increases ($5 \sim 20\%$ of the L-alanine content). This change of the σ_{22} value may be due mainly to neighbouring amino acid sequence effects, but not to the main-chain conformation of polypeptides. The σ_{iso}, σ_{11} and σ_{33} values, on the other hand, do not change at this L-alanine content ($5 \sim 20\%$).

For a series of [Ala*, Val]$_n$ compounds, the stable conformation was found to be the β-sheet form at $\leq 20\%$ L-alanine content (A7-1, A7) and the α-helix form at $\geq 30\%$ L-alanine content (A7-2), as shown in Table 4. An interesting result was that, in the narrow range of L-alanine content (between 20 and 30%), the σ_{22} value exhibits a drastic decrease (*ca.* 9 ppm) as the L-alanine content increases. In contrast, no conformational change occurs (β-sheet form) at $5 \sim 20\%$ L-alanine content, whereas very few changes occur in the values of σ_{22}. This supports the view that σ_{22} is governed mainly by the conformation of copolypeptides and is conformation dependent. As described above, it is generally difficult to estimate the main-chain conformation of a variety of copolypeptides on the basis of σ_{iso} data. However, it is now possible to determine the conformation of copolypeptides on the basis of σ_{22} values, if the ^{15}N-labelled copolypeptide (or natural protein) can be provided. Large changes are seen for the σ_{iso}, σ_{11}, and σ_{33} values (other than σ_{22}) at $5 \sim 20\%$ L-alanine content. These changes may be mainly due to the neighbouring amino acid sequence effects (or higher ordered effects) of copolypeptides. For a series of [Ala*, D-Ala]$_n$, no displacements of σ_{iso}, σ_{11}, and σ_{33} were detected over $5 \sim 20\%$ L-alanine content. The value of σ_{22} is, however, decreased as the L-alanine content increases. This may be ascribed to neighbouring amino acid sequence effects.

Figure 21 shows the diagram of the observed σ_{iso}, σ_{11}, σ_{22}, and σ_{33} data of the Gly* residue of [Gly*, X]$_n$ (Gly* content is nearly 20%). The range of the σ_{22} values of the α-helical [Gly*, X]$_n$ decreases with respect to those of the β-sheet [Gly*, X]$_n$, whereas the range of the σ_{11} and σ_{33} values of the α-helix increases with respect to that of the β-sheet form. The displacement of σ_{11} and σ_{22} of [Gly*, X]$_n$ is very sensitive to the conformational changes of copolypeptides. The σ_{11} and σ_{22} data of the Gly* of the α-helix form and those of the β-sheet form are observed separately, and are quite similar to those of the Ala* of [Ala*, X]$_n$. However, the displacement of the tensor element σ_{33} (parallel to the C′–N bond direction[36,37]) of the α-helix and β-sheet forms is different

from that of the $[Ala^*, X]_n$. This suggests that σ_{33} is related to the side-chain structures of solid polypeptides, although further study is needed to confirm this.

Figures 27 and 28 show the plots of σ_{iso}, σ_{11}, σ_{22}, and σ_{33} values of various $[Gly^*, Ala]_n$ and $[Gly^*, Leu]_n$ against glycine content. It is interesting that the value of σ_{iso} is nearly constant, but the principal shielding tensor components are displaced over a wide range of glycine content ($20 \sim 100\%$). Therefore, these tensor components contain some information about neighbouring amino acid sequence effects as well as conformation. The reason for this is not clear at present.

Figure 22 shows the observed σ_{iso} and σ_{22} data of the Leu* residue of $[Leu^*, X]_n$ (Leu* content is nearly 20%). The range of σ_{22} values of the α-helical $[Leu^*, X]_n$ is smaller than that of the β-sheet $[Leu^*, X]_n$. The σ_{22} values of the Leu* of the α-helix and β-sheet forms are observed separately in the ranges $50 \sim 57$ and $58 \sim 67$ ppm, respectively. Thus, the displacement of σ_{22} of $[Leu^*, X]_n$ is very sensitive to the conformational changes of copolypeptides. The variation of σ_{22} among the α-helical $[Leu^*, X]_n$ is 7 ppm, and that of the β-sheet form is 9 ppm. This result suggests that the σ_{22} value of the Leu* residue may be related to strong neighbouring amino acid sequence effects as well as conformational effects.

Figure 29 shows the plots of σ_{iso} and σ_{22} of various $[Leu^*, Val]_n$, $[Leu^*, Ala]_n$ and $[Leu^*, Gly]_n$ against the L-leucine content. The σ_{iso} value is nearly constant, but the shielding tensor elements are displaced over a wide range of L-leucine content ($20 \sim 100\%$). Therefore, the σ_{22} value contains some information about neighbouring amino acid sequence effects and any higher ordered interactions, as well as conformation-dependent interactions.

In particular, we can now determine the main-chain conformation of various copolypeptides (and some proteins) in the solid state from the σ_{iso} and σ_{22} data by ^{15}N CP/MAS and/or CP-static NMR methods, if the ^{15}N-labelled copolypeptide or ^{15}N-labelled natural protein can be provided. As the relation between the nitrogen shielding and the structures (primary, secondary and higher ordered structures) is clarified in the future, we will be able to get more detailed information on the structure of polypeptides and proteins in the solid state.

Finally, we would like to mention briefly that solid-state ^{15}N NMR has been successfully applied to the structural characterization of natural proteins in addition to solid-state ^{13}C NMR. As there is no space to describe it in detail, we provide some references only.[45,46,54,76–82]

REFERENCES

1. M. Mehring, *Principles of High Resolution NMR in Solids* (2nd edition). Springer-Verlag, Berlin, 1983.

2. P. Granger and R.K. Hains (eds), *Multinuclear Magnetic Resonance in Liquids and Solid-Chemical Applications*. Kluwer Academic Publishers, Dordrecht, 1990.
3. R.G. Griffin, J.D. Ellett, M. Mehring, J.D. Bullitt and J.S. Waugh, *J. Chem. Phys.*, 1972, **57,** 2147.
4. N. Bloembergen and J.A. Rowland, *Acta Met.*, 1953, **1,** 731.
5. M. Witanowoki and G.A. Webb (eds), *Nitrogen NMR*. Plenum, London, 1973.
6. G.C. Levy and R.L. Lichter, *Nitrogen-15 NMR Spectroscopy*. John Wiley & Sons, New York, 1979.
7. G.J. Martin, M.L. Martin and J.P. Govesnard, ^{15}N *NMR Spectroscopy*. Springer-Verlag, Berlin, 1981.
8. B.C. Gerstein and C.R. Dybowski, *Transient Technique in NMR of Solids*. Academic Press, London, 1985.
9. J. Schaefer, R.A. McKay and E.O. Stejskal, *J. Magn. Reson.*, 1979, **34,** 443.
10. J. Schaefer, E.O. Stejskal and R.A. McKay, *ACS Symp. Series*, 1982, **191,** 187.
11. M.M. Maricq and J.S. Waugh, *Chem. Phys. Lett.*, 1977, **47,** 327.
12. M.M. Maricq and J.S. Waugh, *J. Chem. Phys.*, 1979, **70,** 3300.
13. J. Herzfeld and A.E. Berger, *J. Chem. Phys.*, 1980, **73,** 6021.
14. M. Linder, A. Hohener and R.R. Ernst, *J. Chem. Phys.*, 1980, **73,** 4959.
15. M.G. Munowitz, R.G. Bodenhousen and T.H. Huang, *J. Am. Chem. Soc.*, 1981, **103,** 2529.
16. M.G. Munowitz and R.G. Griffin, *J. Chem. Phys.*, 1982, **76,** 2848.
17. J.E. Roberts, S. Vega and R.G. Griffin, *J. Am. Chem. Soc.*, 1984, **106,** 2506.
18. R.A. Haberkorn, R.E. Stark, H. van Willigen and R.G. Griffin, *J. Am. Chem. Soc.*, 1983, **103,** 2534.
19. R.E. Stark, L.W. Jelinski, D.J.Rubin, D.A. Torchia and R.G. Griffin, *J. Magn. Reson.*, 1983, **55,** 266.
20. R.E. Stark, R.A. Haeberkorn and R.G. Griffin, *J. Chem. Phys.*, 1978, **68,** 1996.
21. J.E. Roberts, G.S. Harbison, M.G. Munowitz, J. Herzfeld and R.G. Griffin, *J. Am. Chem. Soc.*, 1987, **109,** 4163.
22. I. Ando and G.A. Webb, *Theory of NMR Parameters*. Academic Press, London, 1983.
23. D.B. Chestnut, in *Annual Reports on NMR Spectroscopy*, Vol. 21 (ed. G.A. Webb), p. 51. Academic Press, London, 1989.
24. *Specialist Periodical Report on NMR*, Vol. 20 (ed. G.A. Webb). Royal Society of Chemistry, London, 1991.
25. S. Kuroki, S. Ando, I. Ando, A. Shoji, T. Ozaki and G.A. Webb, *J. Mol. Struct.*, 1990, **240,** 19.
26. S. Kuroki, S. Ando, I. Ando, A. Shoji and T. Ozaki, *J. Mol. Struct.*, 1991, **245,** 69.
27. M. Witanowski, L. Stefaniak and G.A. Webb, in *Annual Reports on NMR Spectroscopy*, Vol. 24 (ed. G.A. Webb). Academic Press, London, 1991.
28. M. Schindler, *J. Am. Chem. Soc.*, 1988, **110,** 6623.
29. I. Ando, T. Yamanobe, H. Kurosu and G.A. Webb, in *Annual Reports on NMR Spectroscopy*, Vol. 22 (ed. G.A. Webb), p. 206, Academic Press, London, 1990.
30. G. Harbison, J. Herzfeld and R.G. Griffin, *J. Am. Chem. Soc.*, 1987, **109,** 4163.
31. J. Herzfeld, J.E. Roberts and R.G. Griffin, *J. Chem. Phys.*, 1987, **86,** 597.
32. Y. Hiyama, C.H. Niu, J.V. Silverton, A. Bavoso and D.A. Torchia, *J. Am. Chem. Soc.*, 1988, **110,** 2378.
33. M. Munowitz, W.P. Aue and R.G. Griffin, *J. Chem. Phys.*, 1982, **77,** 1686.
34. G.S. Harbison, L.W. Jelinski, R.E. Stark, D.A. Torchia, J. Herzfeld and R.G. Griffin, *J. Magn. Reson.*, 1984, **60,** 79.
35. C.J. Hartzell, T.K. Pratum and G. Drobny, *J. Chem. Phys.*, 1987, **87,** 4324.
36. T.G. Oas, C.J. Hartzell, F.W. Dahlquist and G.P. Drobny, *J. Am. Chem. Soc.*, 1987, **109,** 5962.
37. C.J. Hartzell, M. Whitfield, T.G. Oas and G.P. Drobny, *J. Am. Chem. Soc.*, 1987, **109,** 5966.
38. Q. Teng and T.A. Cross, *J. Magn. Reson.*, 1989, **85,** 439.

39. Q. Teng, L.K. Nicholson and T.A. Cross, *J. Mol. Biol.*, 1991, **218,** 607.
40. L.K. Nicholson, Q. Teng and T.A. Cross, *J. Mol. Biol.*, 1991, **218,** 621.
41. G.R. Marshall, D.D. Beusen, K. Kociolek, A.S. Redlinski, M.T. Leplawy, Y. Pan and J. Schaefer, *J. Am. Chem. Soc.*, 1990, **112,** 963.
42. Y. Pan, T. Gullion and J. Schaefer, *J. Magn. Reson.*, 1990, **90,** 330.
43. Y. Pan and J. Schaefer, *J. Magn. Reson.*, 1990, **90,** 341.
44. G.A. Webb and M. Witanowski, *Proc. Indian Acad. Sci. (Chem. Sci)*, 1985, **94,** 241.
45. T.A. Cross, J.A. Diverdi and S.J. Opella, *J. Am. Chem. Soc.*, 1982, **104,** 1759.
46. T.A. Cross, M.H. Frey and S.J. Opalla, *J. Am. Chem. Soc.*, 1983, **105,** 7471.
47. H.G. Foerster, D. Mueller and H.R. Kricheldorf, *Int. J. Biol. Macromol.*, 1983, **5,** 101.
48. T.H. Huang, W.W. Bachovchin, R.G. Griffin and C.M. Dobson, *Biochemistry*, 1984, **23,** 5933.
49. E.O. Stejskal, J. Schaefer and R.A. McKay, *J. Magn. Reson.*, 1984, **157,** 471.
50. C.N. Matthews, R. Ludicky, J. Schaefer, E.O. Stejskal and R.A. McKay, *Origins Life*, 1984, **14,** 243.
51. T.A. Cross and S.J. Opella, *J. Mol. Biol.*, 1985, **182,** 367.
52. B.S. Choi, J.E. Roberts, J.N.S. Evans and M.F. Roberts, *Biochemistry*, 1986, **25,** 557.
53. J. Schaefer, J.R. Garbow, G.S. Jacob, T.M. Forrest and G.E. Wilson, Jr., *Biochem. Biophys. Res. Commun.*, 1986, **137,** 7361.
54. P.L. Stewart, K.G. Valentine and S.J. Opella, *J. Magn. Reson.*, 1987, **71,** 45.
55. S.O. Smith, S. Farr-Jones, R.G. Griffin and W.W. Bachovchin, *Science*, 1989, **244,** 961.
56. H.J.M. de Groot, S.O. Smith, J. Courtin, E. van den Berg, C. Winkle, J. Lugtenburg, R.G. Griffin and J. Herzfeld, *Biochemistry*, 1990, **29,** 6873.
57. A. Shoji, T. Ozaki, T. Fujito, K. Deguchi and I. Ando, *Macromolecules*, 1987, **20,** 2441.
58. A. Shoji, T. Ozaki, T. Fujito, K. Deguchi, S. Ando and I. Ando, *Macromolecules*, 1989, **22,** 2860.
59. A. Shoji, T. Ozaki, T. Fujito, K. Deguchi, S. Ando and I. Ando, *J. Am. Chem. Soc.*, 1990, **112,** 4693.
60. A. Shoji, T. Ozaki, T. Fujito, K. Deguchi and I. Ando, manuscript in preparation.
61. A. Shoji, T. Ozaki, T. Fujito, K. Deguchi and I. Ando, manuscript in preparation.
62. A. Shoji, T. Ozaki, T. Fujito, K. Deguchi, I. Ando and J. Magoshi, manuscript in preparation.
63. I. Ando, H. Saito, R. Tabeta, A. Shoji and T. Ozaki, *Macromolecules*, 1984, **17,** 457.
64. S. Arnott and A.J. Wonacott, *J. Mol. Biol.*, 1966, **21,** 371.
65. S. Arnott, S.D. Dover and A. Elliott, *J. Mol. Biol.*, 1967, **30,** 201.
66. S. Arnott and S.D. Dover, *J. Mol. Biol.*, 1967, **30,** 209.
67. A. Shoji, H. Katoh, T. Ozaki, S. Kuroki and I. Ando, manuscript in preparation.
68. A. Shoji, T. Ozaki, H. Saito, R. Tabeta and I. Ando, *Macromolecules*, 1984, **17,** 1472.
69. T. Taki, S. Yamashita, M. Satoh, A. Shibata, T. Yamashita, R. Tabeta and H. Saito, *Chem. Lett.*, 1981, 1803.
70. H. Saito, R. Tabeta, A. Shoji, T. Ozaki and I. Ando, *Macromolecules*, 1983, **16,** 1050.
71. H. Saito, R. Tabeta, I. Ando, T. Ozaki and A. Shoji, *Chem. Lett.*, 1983, 1437.
72. H.R. Kricheldorf and D. Mueller, *Macromolecules*, 1983, **16,** 615.
73. H. Saito and I. Ando, in *Annual Reports on NMR Spectroscopy*, Vol. 22 (ed. G.A. Webb), p. 209. Academic Press, London, 1989.
74. T. Miyazawa, *Poly-a-Amino Acids* (ed. G.D. Fasman), Chap. 2 and references therein. Marcel Dekker, New York, 1967.
75. K. Ito, H. Katabuchi and T. Shimanouchi, *Nature, New Biol.*, 1972, **239,** 42, and references therein.
76. C.M. Gall, T.A. Cross, J.A. DiVerdi and S.J. Opella, *Proc. Natl. Acad. Sci. USA*, 1982, **79,** 101.
77. L. Mueller, M.H. Frey, A.L. Rockwell, L.M. Gierasch and S.J. Opella, *Biochemistry*, 1986, **25,** 557.
78. L.K. Nicholson, F. Moll, T.E. Mixon, P.V. LoGrasso, J.C. Lay and T.A. Cross, *Biochemistry*, 1987, **26,** 6621.
79. J.A. Killian, L.K. Nicholson and T.A. Cross, *Biochim. Biophys. Acta*, 1988, **943,** 535.

80. D.M. Schneider, R. Tycko and S.J. Opella, *J. Magn. Reson.*, 1987, **73,** 568.
81. M.J. Bogusky, R.A. Schiksnis, G.C. Leo and S.J. Opella, *J. Magn. Reson.*, 1987, **72,** 186.
82. G.B. Fields, C.G. Fields, J. Petefish, H.E. VanWart and T.A. Cross, *Proc. Natl. Acad. Sci. USA*, 1988, **85,** 1388.